COO-1749-24

A SEARCH FOR A CP-NONCONSERVING ASYMMETRY IN THE DECAY $K_L^0 \to \pi^+\pi^-\pi^0$

by

Lawrence B. Levit

Submitted in partial fulfillment of the requirements

for the Degree of Doctor of Philosophy

Thesis Advisor: Dr. W. A. Blanpied

Department of Physics

CASE WESTERN RESERVE UNIVERSITY

January 1971

DISCLAIMER

A SEARCH FOR A CP-NONCONSERVING ASYMMETRY IN THE DECAY $K_L^o \rightarrow \pi^+\pi^-\pi^o$

Abstract

by

LAWRENCE B. LEVIT

The purpose of this experiment was to test CP symmetry in the decay $K_L^o \rightarrow \pi^+\pi^-\pi^o$. A search was made for a charge asymmetry revealing itself as a difference between the π^+ and π^- transverse momentum spectra. The experimental configuration was three hodoscopes in line and a momentum analyzing magnet.

The experimental limit set by this experiment was calculated from the data for which both charged π mesons were detected, and one γ-ray from the π^o decay was identified. This constitutes 400,000 events. The experimental data were analyzed by a Monte Carlo fitting procedure. The best value obtained for the CP violating parameter, $\sigma\pm$, was 0.0001 ± 0.0009. Estimates of all biases that could mask the asymmetry are included in the uncertainty quoted above.

Two previous experiments[A,B] have shown no asymmetry to a precision of 0.02, and one experiment exhibited a 2-1/2 standard deviation effect of 0.04.[C]

The result of this experiment is consistent with CP invariance.

A. B. M. K. Nefkens, A. Abashian, R. J. Abrams, D. W. Carpenter, G. P. Fisher, and J. H. Smith, Phys. Rev. 157, 1233 (1967).

B. R. C. Smith, L. Wang, M. C. Whatley, G. T. Zorn, and J. Hornbostel, Bull. Am. Phys. Soc. 13, 586 (1968).

C. H. W. K. Hopkins, T. C. Bacon, and F. R. Eisler, Phys. Rev. Letters 19, 185 (1967).

TABLE OF CONTENTS

LIST OF FIGURES AND THEIR CAPTIONS

LIST OF FIGURES AND THEIR CAPTIONS

LIST OF TABLES

I. INTRODUCTION

In order to simplify theoretical calculations of elementary particle interactions, a number of assumptions were made. Specifically they were: symmetry of the interaction Hamiltonian under the operations parity reversal (P), charge conjugation (C), and time reversal (T). These assumptions were indeed born out for the case of strong interactions, but the weak interactions were found to be more complex.

Observation of K^+ decays in 1955-1956 (referred to as the θ-τ puzzle) led Lee and Yang to question the validity of parity conservation.[1] They found that no experimental evidence existed for parity conservation in weak interactions. Their suggestions were confirmed in 1957 by a series of experiments including Mrs. Wu's experiment on nuclear β decay of Co^{60}.[2]

Soon after the downfall of the parity symmetry law, the violation of charge conjugation in weak interactions was also observed. The complicating factors led particle theorists to look for other simplifying assumptions. In 1957 Landau,[3] and also Lee and Yang[4] proposed that weak interactions exhibited symmetry under the combined operation PC.

The K_L^o K_S^o system was hypothesized in 1955 by Gell-Mann and Pais.[5] These two particles were defined as eigenstates of C, but in 1958 the formalism was changed, and they were defined as PC eigenstates.

The K_S^o AND K_L^o decays were used for experimental tests of

PC invariance. Specifically the theory predicts the short lived K° may decay into 2π mesons, but the long lived one cannot. In 1958 the absence of $K_L^\circ \to \pi\pi$ was determined to 1%[6] and in 1961 to 0.3%,[7] thus putting the theory on a sound basis.

In 1964, Christenson et al.,[8] detected the decay $K_L^\circ \to \pi^+ + \pi^-$ forbidden by PC invariance. The result of the experiment was certainly surprising first because the violations of both C and P were maximum, and second, no other examples of the violation were found.

A number of hypotheses were put forward (these will be discussed below) concerning the violation of PC, however, the number and accuracy of experiments done to date does not strongly rule out or reinforce any of these theories.

The experiment described in this thesis was performed to aid to the phenomenology of PC, and to help in the sorting out of various theories proposed. A charge asymmetry was searched for in the decay $K_L^\circ \to \pi^+\pi^-\pi^\circ$. Because of the magnitude of the PC violation in the 2π decay, it was expected that any PC violation would be slight, so very good statistics were necessary. This requirement was fulfilled because this was a counter experiment.

This experiment was discussed in an earlier publication[D].

[D] W.A. Blanpied, L.B. Levit, E. Engels, M. Goitien, T. Kirk, D.G. Ryan and D.G. Stairs, Phys. Rev. Letters 21, 24 (1968).

II. THEORY

The K° and $\bar{K}^\circ$ are not eigenstates of the weak Hamiltonian, H_w. A pair of linear combinations

$$|K_S^\circ\rangle = (|K^\circ\rangle + r|\bar{K}^\circ\rangle)/(1 + r^2)^{\frac{1}{2}}$$

$$|K_L^\circ\rangle = (|K^\circ\rangle - r|\bar{K}^\circ\rangle)/(1 + r^2)^{\frac{1}{2}}$$

are eigenstates of H_W. Here r is related to the off diagonal elements of the mass squared matrix, W by[9]

$$r = \left[\frac{\langle\bar{K}^\circ|W|K^\circ\rangle}{\langle K^\circ|W|\bar{K}^\circ\rangle}\right]^{\frac{1}{2}}$$

If one takes $r = 1$, the states $|K_S^\circ\rangle$ and $|K_L^\circ\rangle$ are also eigenstates of PC with eigenvalues +1 and -1 respectively ($PC|K^\circ\rangle = + |\bar{K}^\circ\rangle$ has been used).

The 2π state must be even under CP. Since the π mesons satisfy Bose statistics, the wave function must be even under total exchange. Under the operation PC,

$$\pi^+ \to \pi^- \qquad \pi^- \to \pi^+$$

$$\vec{r}_+ \to \vec{r}_- \qquad \vec{r}_- \to \vec{r}_+$$

so we have total exchange and

$$PC|\pi^+\pi^-> = + |\pi^+\pi^->.$$

Thus, the decay

$$K_S^\circ \rightarrow \pi^+\pi^-$$

is allowed by the conservation of CP but

$$K_L^\circ \rightarrow \pi^+\pi^-$$

is forbidden.

In 1964 the forbidden 2π decay was first observed.[10] The branching ratio is only 1.6×10^{-3}.[11] The detection of this decay is evidence of PC violation. The existence of this decay means that at least one CP violating virtual interaction exists connecting the states K° to $\bar{K}^\circ$ to each other and to themselves.

A number of theoretical frameworks have been proposed to deal with the violation. Sachs[12] suggests that the observed decay may be an "indirect manifestation of a maximal CP violation in the leptonic interactions of the K° meson". The theory indicates that the existence of the 2π decay channel arises from $r \neq 1$ rather than a difference between the $K^\circ \rightarrow 2\pi$ and $\bar{K}^\circ \rightarrow 2\pi$ rates. The cause of the deviation of r from unity is predicted to be due to maximal violation of CP in leptonic decay modes.

The theory requires further that the amplitude for $\Delta S = -\Delta Q$ be on the order of the $\Delta S = \Delta Q$ amplitude but out of phase by $\pi/2$.

An alternative theory[13] put forth by Truong assumes that the K° decays which satisfy the $\Delta I = 1/2$ rule do conserve CP, but the $\Delta I = 3/2$ decays are not CP invariant. The ratio of $K^\pm \to \pi^\pm + \pi^\circ$ to $K_S^\circ \to \pi^+ + \pi^-$ decay rates was used to determine the strength of the $\Delta I = 1/2$ selection rule. For these decays, $\Delta I > 1/2$ and $\Delta I = 1/2$ respectively. Using the ratio of $K_L^\circ \to 2\pi$ to $K_S^\circ \to 2\pi$ the value of r was calculated to be .995, very close indeed to unity. This implies a charge asymmetry in the leptonic decay of the K_L° of 0.4%.

Lee and Wolfstein's approach[14] is to assume that the weak Hamiltonian is made up of two parts

$$H_W = H_G + H_F$$

where H_G is the usual CP invariant Hamiltonian which satisfies $|\Delta S| < 2$ and H_F is an additional interaction which does not conserve CP. The two terms are characterized by coupling constants F and G.

There are several possibilities for H_F leading to different selection rules. If, for example H_F satisfies $|\Delta S| = 1$, then one would expect

$$\frac{F}{G} \sim \left[\frac{R(K_L^\circ \to \pi^+\pi^-)}{R(K_S^\circ \to \pi^+\pi^-)}\right]^{\frac{1}{2}} \sim 10^{-3}$$

To date, however, no such CP violation has been found in $|\Delta S| = 1$ decays.

A second possibility is that H_F satisfies $|\Delta S| = 2$. In this case, transitions of the sort $K^\circ \leftrightarrow \bar{K}^\circ$ could occur. Then, a transition of the sort $K_L^\circ \to K_S^\circ$ would be possible. If this were the case, one would expect

$$\frac{R(K_L^\circ \to \pi^+\pi^-)}{R(K_L^\circ \to \pi^\circ\pi^\circ)} = \frac{R(K_S^\circ \to \pi^+\pi^-)}{R(K_S^\circ \to \pi^\circ\pi^\circ)}$$

This is not the case.[15,16]

A theory of several authors[17,18] is that C invariance is violated in strong interactions. Since conservation of parity is so well verified, this would imply that CP is violated for strong interactions. This could cause the $K_L^\circ \to 2\pi$ effect by virtue of the K°'s virtual (strong) interactions.

Cabibbo has suggested that in many cases, C violating effects may be severely limited in magnitude by the CPT theorem and parity conservation. He points out, however, that in some complex cases, a C noninvariant effect would not necessarily be so limited.

If indeed there were a violation of C in strong interactions, the $K_L^\circ \to 2\pi$ effect would not be a surprise. Such a violation of C would be expected to be small judging from the magnitude of $K_L^\circ \to 2\pi$. It is interesting to note that tests of C invariance in hadron interactions have not yet been made to a sufficient pre-

cision to confirm or deny the theory.[19]

In this experiment a search was made for CP violations in the decay

$$K_L^\circ \rightarrow \pi^+\pi^-\pi^\circ$$

Such a violation would reveal itself in a charge asymmetry, for example, a difference in the kinetic energy spectra of the 2 charged π mesons. This can be seen as follows: Suppose PC is a constant of the motion. Then the three pion state would be an eigenstate of PC. Any pion state can be broken down into states of definite values of PC depending on the value of the isospin.[20] Operating on a state with P has the effect on momentum

$$\vec{p}_i \rightarrow -\vec{p}_i. \quad i = 1, 2, 3$$

Here the subscript i stands for the positive, negative or neutral meson. Operating with C interchange the π^+ and π^- charge indices. Then the combined action of P and C on the 3π state is

$$PC\Psi^{\pm}(\pi^+(\vec{p}^+,E^+),\pi^-(\vec{p}^-,E^-),\pi^\circ(\vec{p}^\circ,E^\circ))$$

$$= \pm\Psi^{\pm}(\pi^-(-\vec{p}^+,E^+),\pi^+(-\vec{p}^-,E^-),\pi^\circ(-\vec{p}^\circ,E^\circ)) \qquad (1)$$

Here the $\pm$ represents the eigenvalue of PC.

Suppose the 3 pion wave function, ϕ, is not an eigenstate of PC, but rather, a linear combination of PC even and PC odd terms:

$$\phi(\pi^+(\vec{p}^+,E^+),\pi^-(\vec{p}^-,E^-),\pi^\circ(\vec{p}^\circ,E^\circ)) = \Psi^+(\pi^+(\vec{p}^+,E^+),\pi^-(\vec{p}^-,E^-),\pi^\circ(\vec{p}^\circ,E^\circ))$$

$$+ a\Psi^-(\pi^+(\vec{p}^+,E^+),\pi^-(\vec{p}^-,E^-),\pi^\circ(\vec{p}^\circ,E^\circ))$$

Here a is a constant. For such an admixture,

$$|PC\phi(\pi^+(\vec{p}^+,E^+),\pi^-(\vec{p}^-,E^-),\pi^\circ(\vec{p}^\circ,E^\circ)| = |\phi(\pi^+(-\vec{p}^-,E^-),\pi^-(-\vec{p}^+,E^+),$$

$$\pi^\circ(-\vec{p}^\circ,E^\circ))| \neq |\phi(\pi^+(\vec{p}^+,E^+),\pi^-(\vec{p}^-,E^-),\pi^\circ(\vec{p}^\circ,E^\circ))| \qquad (2)$$

This inequality is due to interference of the even and odd PC eigenstates.

According to Equation 1, if the 3 pion wave function is an eigenstate of PC, the π^+ and π^- energy spectra are identical. Equation 2 indicates that if the 3 pion wave function is not an eigenstate of PC, there will be a difference in the π^+ and π^- energy spectra. Thus a $\pi^+\pi^-$ energy asymmetry implies a PC violation.

The 3π final state can have isospin, I, of 0, 1, 2 or 3 since the pion has isospin 1. These possible states are even for even I and odd for odd I. Since the K_L° has isospin 1/2 and is odd

under CP, the $I = 1$ three π state conserves CP and satisfies the $|\Delta I| = 1/2$ rule. Also, the $I = 0$ three π state would also admit the $|\Delta I| = 1/2$ rule, but not CP conservation. Finally, the $I = 2$ state has $|\Delta I| = 3/2$ and does not conserve CP. It is assumed that the $I = 3$ state does not contribute to $K_L^\circ \to \pi^+\pi^-\pi^\circ$ since it would require $|\Delta I| = 5/2$. Then, a CP violation would give a $\pi^+\pi^-$ energy asymmetry by interference between the CP conserving $I = 1$ state and the CP violating $I = 0$ and $I = 2$ final states. If, indeed, Truong's theory[21] is correct, the $I = 0$ final state does not contribute.

A calculation of the magnitude of the energy asymmetry requires estimates of the magnitudes of various 3π decay amplitudes which depend upon centrifugal barriers, amount of CP violation and validity of the $|\Delta I| = 1/2$ rule.

A measure of the energy asymmetry between the charged π mesons is

$$\alpha = \frac{N_+ - N_-}{N_+ + N_-}$$

Here $N_\pm$ is the number of events for which the $\pi^\pm$ had greater energy. Estimates of this parameter range from[22] 10^{-5} to[23] 2.7%. The low estimate is simply a carry over of the CP violation amplitude observed in $K_L^\circ \to 2\pi$. The higher estimate is that predicted by Truong's theory of maximal leptonic violation of CP. Two pre-

vious experiments[24,25] have shown no asymmetry at the 2% level and one experiment[26] exhibited a 2 1/2 standard deviation effect of 4%.

A useful parameterization that was used in this analysis is the "linear matrix-element approximation.[11,27] The final state of the three π mesons can be described by two independent parameters X and Y. These are defined as

$$Y = (2\,T_o - T_{max})^{M_K/M_\pi{}^2}$$

$$X = (T_+ - T_-)^{M_K/M_\pi{}^2}.$$

Here $T_{\pm\atop o}$ is the kinetic energy of the $\pi^{\pm\atop o}$, M_K is the mass of the neutral K, M_π is the mass of the π meson and T_{max} is the maximum kinetic energy kinematically allowed a π meson.

The matrix element, then, can be expanded as

$$M(X,Y) = a + b\,X + cY + \text{higher order terms.}$$

Here a, b and c are constants. The linear approximation then uses only the first order terms:

$$M(X,Y) \approx a + bX + cY$$

and

$$M^2(X,Y) \approx a^2 + 2abX + 2acY.$$

Again, higher order terms have been dropped. Then with

$$\sigma_{\pm} = b/a$$

$$\sigma_{o} = c/a,$$

$$M^2(X,Y) = a^2(1 + \sigma_{\pm}X + \sigma_{o}Y)$$

The constant a^2 determines the rate of the decay and it is of no consequence to this analysis. The quantity σ_o is the so called slope parameter and is a measure of the variation of the density of the Dalitz Plot between the charged π mesons and the neutral π meson.

The quantity $\sigma_{\pm}$, the CP violating parameter, is a measure of the energy asymmetry between the π^+ and π^-. A non-zero value of $\sigma_{\pm}$ implies a violation of CP asymmetry.

III. APPARATUS

A. Synopsis

One of the external particle beams from the Alternating Gradient Syncrotron at Brookhaven National Laboratory was incident upon the apparatus used in this experiment. See Figure 1. The beam consisted of K_L° mesons (the particles whose decays were to be studied) as well as neutron contamination. In order to identify a decay as

$$K_L^\circ \rightarrow \pi^+\pi^-\pi^\circ,$$

The two charged π mesons had to be detected as well as the gamma rays from the essentially instantaneous decay

$$\pi^\circ \rightarrow 2\gamma.$$

The apparatus is shown in Figure 2.

The charged π's were detected by 3 hodoscopes made of 16,8 and 12 plastic scintillator strips. The three hodoscopes were perpendicular to the beam direction and placed one behind the next so that the 2 charged π mesons would cause 2 hodoscope elements in each plane to fire. A large magnet between the second and third hodoscopes bent the charged particles. The particles' paths could be reconstructed from the knowledge of which counters had fired and thus, the momentum of the charged π mesons could be measured.

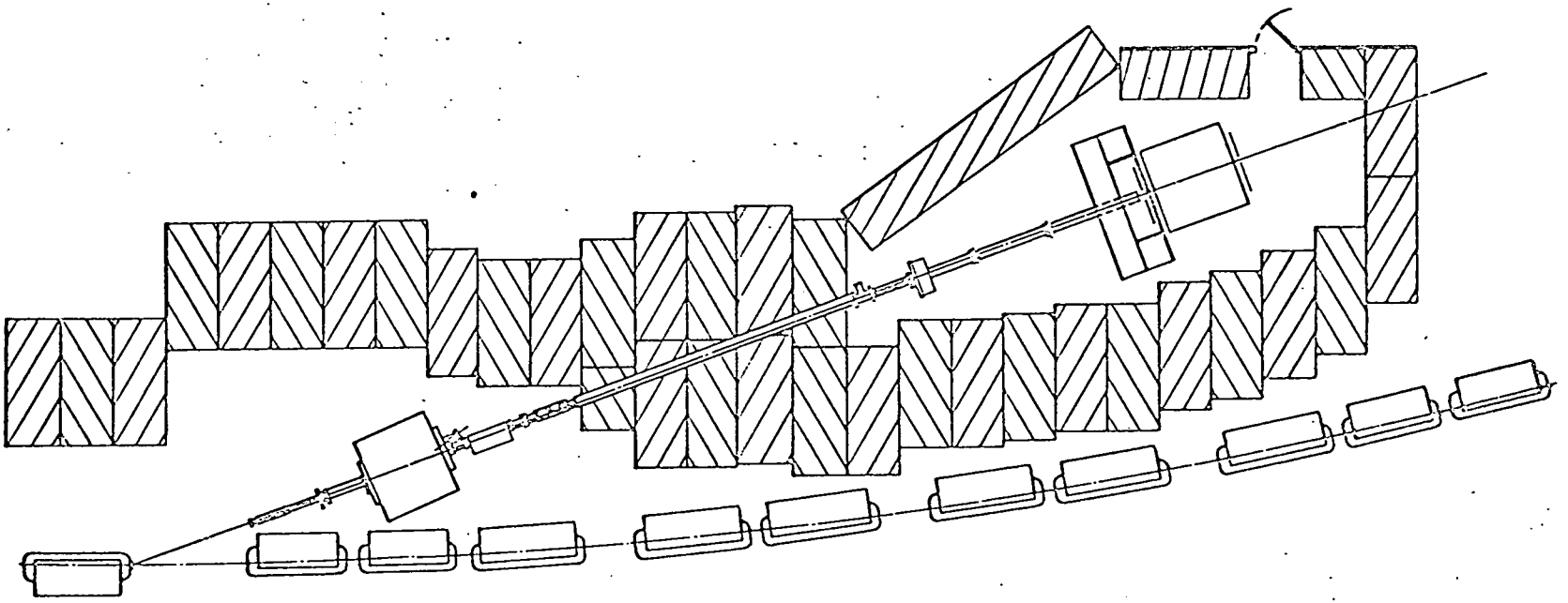

Figure 1

6'

The Floor Plan

The gamma rays from the π^o decay were detected by the use of four shower counters placed upstream of the hodoscopes. These four dectectors were placed parallel to the beam direction such that the beam passed through a sort of tunnel.

In order to guarantee that the particle whose decay was being studied was neutral, a charged particle detector was placed upstream of the apparatus so that a firing of this detector could be used to veto an event during which this counter had been on.

Thus, the decay of interest was completely determined by 2 trajectories in the hodoscopes, 2 of the 4 gamma counters turned on and the charged particle veto counter off.

As mentioned above, the beam also contained neutrons. The interaction of the neutrons could cause false triggers of the apparatus. These false triggers were of concern because they could conceivably have been asymmetric so that an erroneous result would have been obtained. For this reason, the decay region was filled with SF_6, a very heavy gas, during part of the running of the experiment. An estimate of the effects of neutron interactions could thus be obtained by looking at the counting enhancement due to the extra matter in the beam.

B. The Beam

The apparatus used was designed by Bennett et al., for use in an earlier experiment[28] and was modified for use in the present ex-

periment. The beam was produced on a thin beryllium wire internal target (target G 10) by the proton beam of the Alternating Gradient Synchrotron at Brookhaven National Laboratory. It was directed 20 degrees inward from the synchrotron beam. Its geometry is shown in Figure 1. Three brass collimators of rectangular cross section were used to define the beam. The internal faces of the collimators lay on common pyramid whose apex was at the center of the target. The distances of the three collimators from G 10 target were, 3.7, 9.8 and 18.4 meters respectively. The exit opening of the last collimator was 20.8 cm. high and 13.6 centimeters wide. Before traversing the collimators the gamma ray flux was attenuated by allowing the beam to pass through 1.9 cm. of lead and 2.5 cm. of Heavimet (primarily tungsten) a total of 10 radiation lengths. Between the first and second collimators was a large AGS 18D72 sweeping magnet used to bend charged particles from the beam. The current through the magnet was maintained at least three times the value below which an enhancement to 2-fold coincidence rates between hosocopes was noted. A veto scintillator was placed so the entire beam cross section was covered. The efficiency of this counter was measured and found to be in excess of 99 percent for charged particles. Thus, the efficiency for detecting at least one of a charged pair was essentially 1 and although the beam contained some charged particles created downstream of the target, they were effectively vetoed.

The beam generated was one of neutral particles and was well collimated. The distance from the target to the apparatus was 20.4 meters so that the short lived particles decayed in flight leaving a beam of only neutrons, gamma rays, and long lived K-mesons. The fact that there was no contamination of other neutral particles can be easily shown. The highest energy particles of a given half life travel the farthest. At 4 Bev/c incident K° momentum the intensity of the AGS neutral beam was down by a factor of 70 from its maximum value at approximately 1.4 BeV/c. Thus 4 BeV/c is a reasonable choice for the maximum of the K° beam momentum. This being the case, the mean distance traveled before decay was only 25 centimeters, 1/100 the total distance to the apparatus. Thus it is clear that there were no particles in the beam except neutrons K_L°'s and photons. The contamination of the beam by neutrons was a serious problem and the treatment will be described below. The photons in the beam did not represent the same problem. They were attenuated by the ten radiation lengths of lead. The β particles generated by the gamma flux were swept out of the beam by the sweeping magnet (see below).

One half radiation length of lead and later one of steel was placed in the beam to enhance the counting rate due to gamma rays. The counting rate of charged pairs relative to the beam intensity did not show an increase. The measurements were made to an accuracy of 1% and did not include electron discrimination. An upper

limit can be set on the fraction of gamma induced counts using this data. Since the matter in the beam was $< 10^{-3}$ radiation lengths, the fraction of gamma induced counts was less than 1 in 10^5.

In order to avoid interactions between the beam and matter, the beam traversed vacuum for the entire distance from the first collimator to the front veto except for the region of gamma attenuator. Any charged particles created in the attenuator would have been swept out of the beam direction by the sweeping magnet. Any uncharged particles created would have either been K_L^o's, neutrons, photons or would have decayed well before reaching the sweeping magnet.

The geometrical optics of the collimators defined the size of the beam to be 14.5 centimeters wide by 22.2 centimeters high at the upstream end of the apparatus and 16.0 centimeters wide by 24.2 centimeters high at the down stream end of the decay region. The beam diverged only ten percent as it traversed the apparatus.

C. The Floor Plan

Figure 2 is a diagram of the apparatus used in this experiment. Because of the high incident K^o momentum and the low Q (82 MeV) of the reaction, the mean opening angle between a charged π-meson and the beam direction was on the order of 6 degrees. Thus the apparatus was very long and narrow, consequently, Figure 2 has been considerably foreshortened.

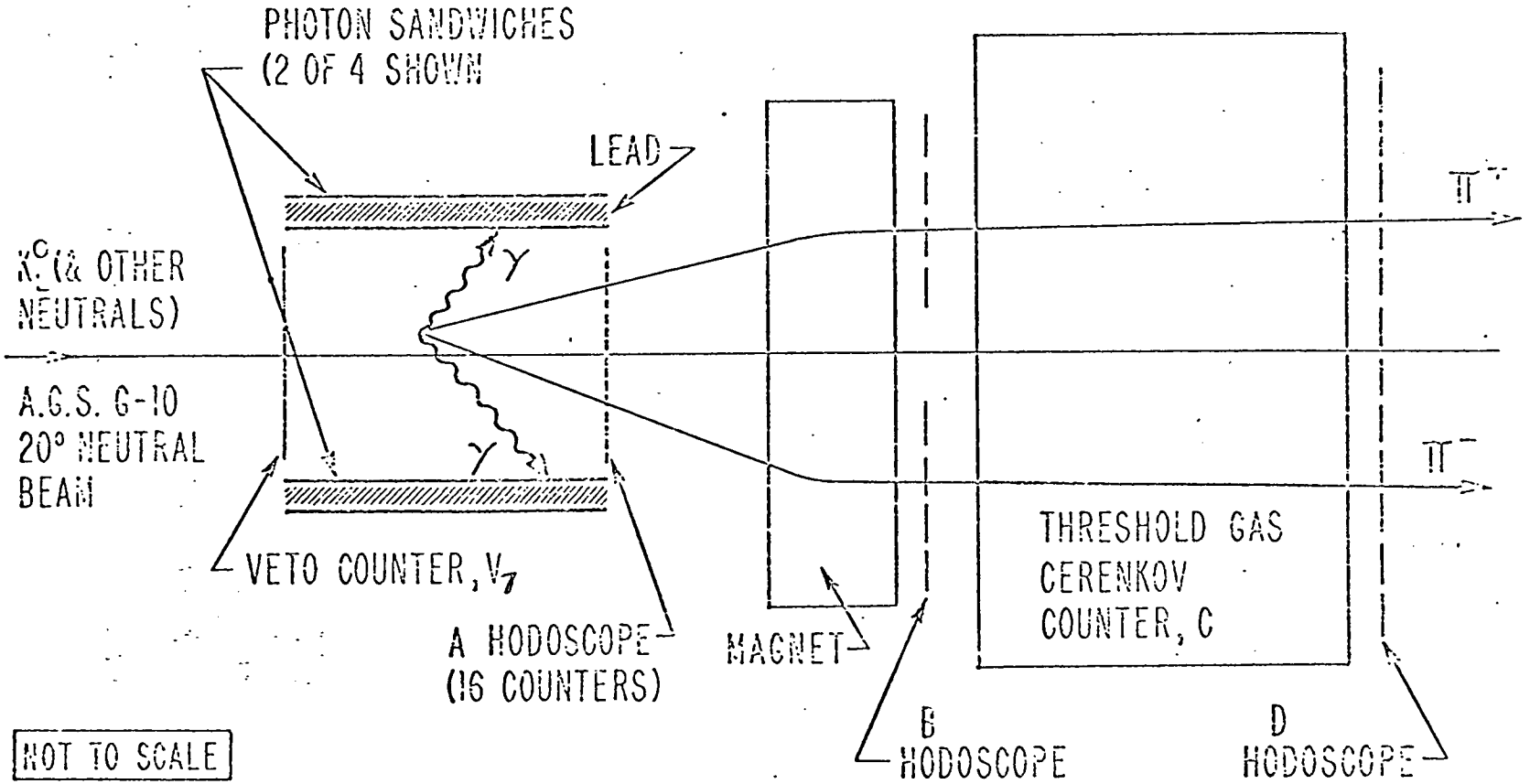

Figure 2

Diagram of the Apparatus

The π^+ and π^- trajectories were defined by three hodoscopes of plastic scintillator, A, B, and D. They contained 16, 8 and 12 vertically oriented counters respectively. The A hodoscope can be seen in Figure 3, B in Figure 6 and D in Figure 5. To contend with the problem of interactions of the charged particles with the counters, the A and B hodoscopes were constructed of very thin plastic .10 mm thick. The counters were all light shielded by thin aluminum foil .025 mm thick. Since interactions in the D hodoscope would not send particles downstream to other counters, these counters were made somewhat thicker, 0.3 mm.

Scintillation light from each of the hodoscope elements was directed to a 2 inch RCA 8575 photomultiplier via a lucite light pipe. Each of the tubes was magnetically shielded by 0.06 cm of mu metal, 0.3 cm of Netic-Conetic shielding and 0.95 cm of iron. Signals from the A and B hodoscopes were amplified with x10 Chronetics 103 amplifiers. The signals were clipped to 5 ns. Because of the high counting rates, the last 3 stages of each tube were driven by booster supplies as were all photomultipliers in this experiment.

In order that a reasonably accurate reconstruction of the decay point be possible, it was necessary to use a large number of narrow counters for the A hodoscopes. This was due to the fact that the A hodoscope was the downstream boundary of the decay region and thus the counters forming this hodoscope subtended the

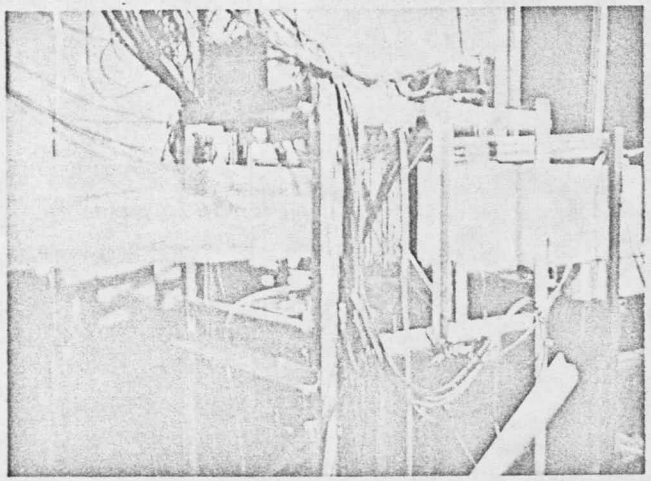

Figure 3 The A Hodoscope

Figure 4
The Electronics

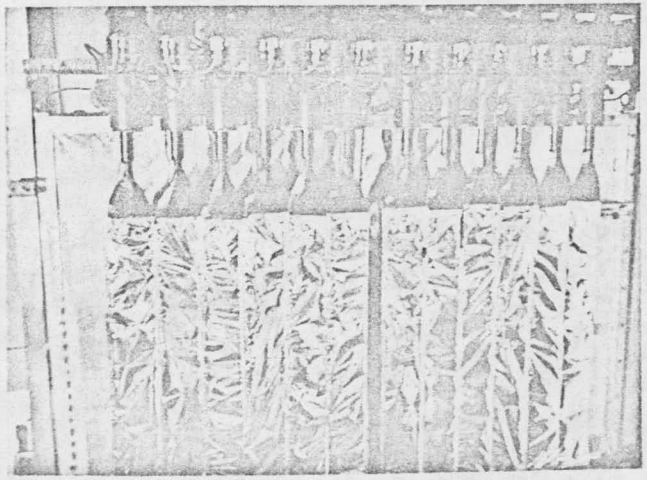

Figure 5 The D Hodoscope

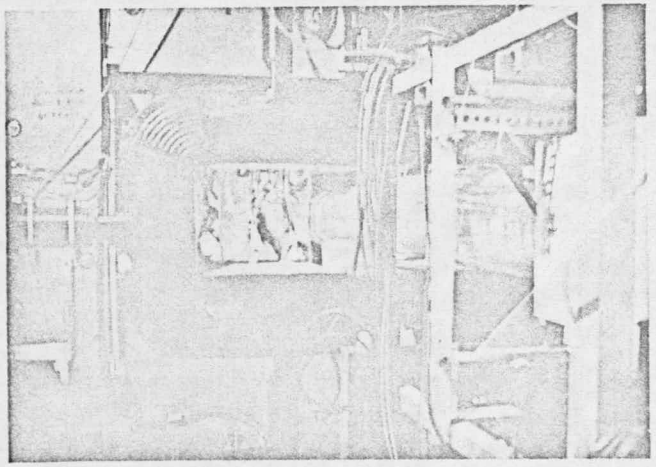

Figure 6 The B Hodoscope

largest solid angle per unit counter dimension of all counters. For this reason, 16 counters of width 1 inch were used. Thus, since the beam was approximately 6 inches across, the entire range of the beam was covered and even the π-mesons emitted at relatively large angles to the beam direction would pass through the apparatus and be detected. The size requirements for the B and D hodoscopes were not as stringent because they were farther from the decay region. For this reason, only 8 counters of width 5.5 inches were used for the B hodoscope. The size of the counters was determined by considerations described below.

A wide gap momentum analyzing magnet was placed between the B and D hodoscopes. It had a vertically oriented field so a transverse momentum kick was delivered to the charged particles. Knowledge of which three counters had fired is sufficient for reconstructing the horizontal component of the particle's momentum vector and the horizontal coordinates of the decay vertex. The size of the C and D counters was determined subject to the condition that the maximum possible (see Figure 7) deflection of a π passing from the B to D planes be less than 1 1/2 counter widths. Thus a logical constraint could be placed on the data to eliminate spurious counts. This constraint is called angle logic and is signified by $\}$.

In order to avoid extraneous counts due to interactions between particles and the magnet, the entire magnet gap was covered

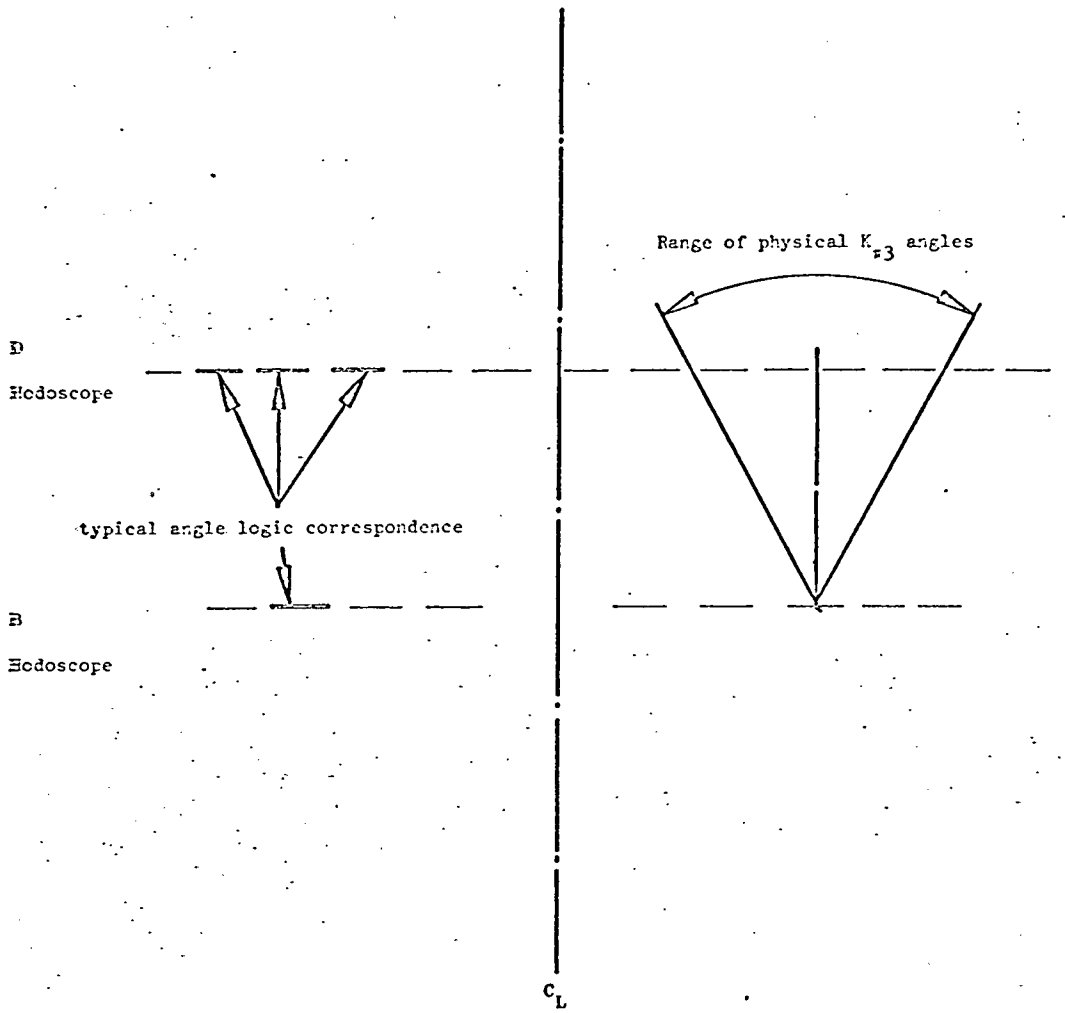

Angle logic constraint of hodoscopes

Figure 7

by 6 counters used to veto scatters from the magnet. These counters were called $V_1 - V_6$.

An ethylene gas (C_2H_4) Čerenkov detector was placed between the B and D hodoscopes. This detector was designed to differentiate between electrons and all other types of charged particles. This is possible because Čerenkov light intensity is velocity dependent rather than momentum or energy dependent. The condition for threshold of Čerenkov light is $n \cdot \beta = 1$. Here n is the index of refraction of the gas and β is the ratio of the velocity to the speed of light. Since the index of refraction of the gas is 1.0007 the threshold velocity is 0.9993c. For electrons, this corresponds to an energy of 13 MeV, for muons 2.7 BeV and for π-mesons 3.8 BeV. Thus the detector differentiated between electrons and other charged particles. The efficiency of this detector for electrons can be calculated as follows: the number of photons per unit path length from Čerenkov radiation is

$$\frac{d^2N}{dxd\nu} = \frac{2\pi}{137c}\left(1 - \frac{1}{\beta^2 n^2}\right) \quad (29)$$

Here β is the ratio of the velocity to the speed of light, n is the index of refraction of the medium and ν is the photon frequency. Since the phototubes used in the detector were Amperex 58AVP's, the response of the photocathodes was a standard S-11. Thus if the light collection efficiency is taken as flat at 8%

over the range 3000 to 5000 angstroms for a total path length through the detector of one meter, the average number of photoelectrons generated by an ultra-relativistic electron ($\beta = 1$) was 5. The distribution of photoelectrons is given by the Poisson relation:

$$\text{Prob}(n) = 5^n e^{-5}/n!$$

If no fewer than 2 photoelectrons could be distinguished as a signal, the probability of an electron's passing through undetected is:

$$\text{Prob}(0) + \text{Prob}(1) = 0.04$$

Thus the efficiency was > 95%. The Čerenkov detector contained 8 photomultiplier tubes located for optimal light collection efficiency. The fact that particles emit Čerenkov light at an angle given by $\sin\theta = 1 - \frac{1}{\beta^2 n^2}$ indicates that the range of possible angles is 0 to 2.1°, well directed light. Thus an efficient light collection system was possible employing reflected light off 8 aluminized mirrors and focused onto the photocathodes of the tubes. The 8 tubes were driven at 2700 volts and their unclipped signals were added using an E. G. & G. AN100 mixer, giving a single signal for pulse height analysis.

There was a thin square of plastic scintillator at the up-

stream end of the apparatus located 6 feet from the A hodoscope. This was used to guarantee that any trigger of the apparatus that appeared to be an acceptable event was not caused by charged particles entering the apparatus through the beam port. This veto counter was called V_7. Thus, since the system would not reveal completely defined pair of charged particle trajectories if a count occured after A, the decay region was delineated by V_7 and the A hodoscope.

In order to minimize interactions between the beam (particularly neutrons) with the matter in its path, it would have been advantageous to place the apparatus in an evacuated room. This was of course not technically feasible, so a reasonable approximation would be a low atomic weight gas. Because helium is inert, it is a good safe choice. Polyethylene bags containing helium at one atmosphere were placed in the decay region and between the A and B hodoscopes. In order to correct for the existence of some matter in the beam, a portion of the running time of the experiment utilized a heavy gas, SF_6 (molecular weight is 150) in place of helium. Using the results of the experiment in the SF_6 phase, the existence of any matter in the decay region could be corrected for.

Since the π^o decayed in an unmeasureably short distance ($< 10^{-5}$ cm), only the gamma rays associated with this decay were detected. The gamma counters used were conventional shower coun-

ters using approximately one radiation length of lead to shower the gamma rays. The counters were constructed of a layer of plastic scintillator, a layer of lead and another layer of plastic scintillator. A gamma ray was assumed to have been detected if the first counter was off and the second was on. That is, the gamma ray converted in the lead and the charged pairs caused the second layer to scintillate. The greatest difficulty with such a counter stems from the fact that an event in which both counters are turned on is considered to be an event due to a charged particle rather than a gamma ray. Thus, the first counter may be thought of as a veto counter for charged particles. This places rather severe limitations upon the acceptable locations of the gamma counters. They cannot be placed so that the charged π-mesons pass through them. Thus, the most logical location, behind the apparatus, is ruled out. For this reason, the four gamma counters were placed around the decay region. They formed a sort of gamma tunnel around the decay region so that gamma rays emitted at large angles would pass through the tunnel detectors but the charged π-mesons would not.

D. The Electronics

The electronics are shown in Figure 4. The resolving time of this experiment was on the order of 5 nanoseconds so care had to be taken to keep the cable lengths consistent with correct counter timing. The techniques employed in counter timing will be described below.

The anode signals of the hodoscope gamma counter and veto counter photomultipliers were clipped to 5 ns. and fed into Chronetics 101 discriminators. As mentioned above, the outputs of the A and B hodoscopes were also amplified. Before the signals were fed into the discriminators, the signals were all timed with respect to each other at a common panel called the isochronous panel. Each of the signals could be passed through or a test pulse could be injected.

The fast logic pulse was generated using standard bin type logic. The requirement for a trigger of the fast logic was

$$T = (B_L \geq 1)\ (B_R \geq 1) \cdot (\text{During beam spill}) \cdot (\text{System Not busy})$$

Here B_L and B_R are the number of B hodoscope elements that were on for the left and right sides respectively. Determination that the beam spill was on was done via a digital clock gated on by the AGS magnet pulse. The clock produced a DC level which vetoed events between AGS beam spills.

The trigger, T, activated the input control unit, TGI (Trigger Gate Initiate). This unit cleared the registers (to be discussed below) and strobed them on again. The widow widths of the strobe pulses were set by clipping cables to be 20 nanoseconds for all hodoscope constituents and gamma counter halves

and 30 nanoseconds for the veto counters. The outputs of all discriminators to the registers were delayed by 80 nanoseconds to bring the pulses into time with the strobe windows.

The status of the hodoscope elements, gamma counter elements and veto counters was stored as DC levels in a series of registers. This occured when TGI strobed on the registers. Once this information was stored, it was interrogated by DC logic. Levels were set for the left and right sides of the B and D hodoscopes and the entire A hodoscope for the conditions = 0, =1, = 2, $\geq$ 1 and $\geq$ 2 elements on. The complementary levels were also available. Also, logic levels for angle logic were generated.

There were 15 logic busses to all of which 10 selected logic levels as described above were supplied in parallel. With the inclusion of six external logical inputs, these busses could be used to generate up to a 16-fold logical combination. This combination could be set by a series of front panel switches each of which could be set to true, false or ignore.

One of these modules was used to generate the event decision level, E. This level was interrogated by the trigger pulse sufficiently delayed, TD, at the output trigger generator TGO (Trigger Gate Output). The logical constraint used was

$$TGO = TGI \cdot (A \geq 2) \cdot (D_{left} \geq 1) \cdot (D_{right} \geq 1)(V_7 = 0) \cdot (G \geq 1)$$

Here $G \geq 1$ signifies that at least one of the eight gamma scintillators had a light pulse during the event and $V_\gamma = 0$ signifies that the upstream charge anti-coincidence had no pulse. The gamma restriction was included to limit the rate of data taking. The event requirement used was less restrictive than one would want to analyze only $K_{3\pi}$ events. This specific requirement was used in order to be able to later study various backgrounds.

In addition to event logic levels, the other logical levels were interrogated with TD and the results were counted on scalers independent of the event level. Also, 6 additional logical levels were generated to facilitate easy analysis and and to check for malfunctions in the system.

If an event was to be recorded, the TGO unit extended the dead time (unit busy pulse) to 22 μsec, initialized the area to height and analog to digital convertors used with the Čerenkov counter and the ADC used with the beam intensity telescope and requested the data handler write the event in its core memory. The timing of the logic system is shown in Figure 8.

The BNL data handler consisted of a 4096 word magnetic core memory and associated control circuitry. The words in this memory were 36 bits. At the end of each beam spill, the data handler was interrogated to see if the number of events recorded in the core was greater than a preset minimum. This minimum was adjustable according to conditions during the experiment. When the minimum

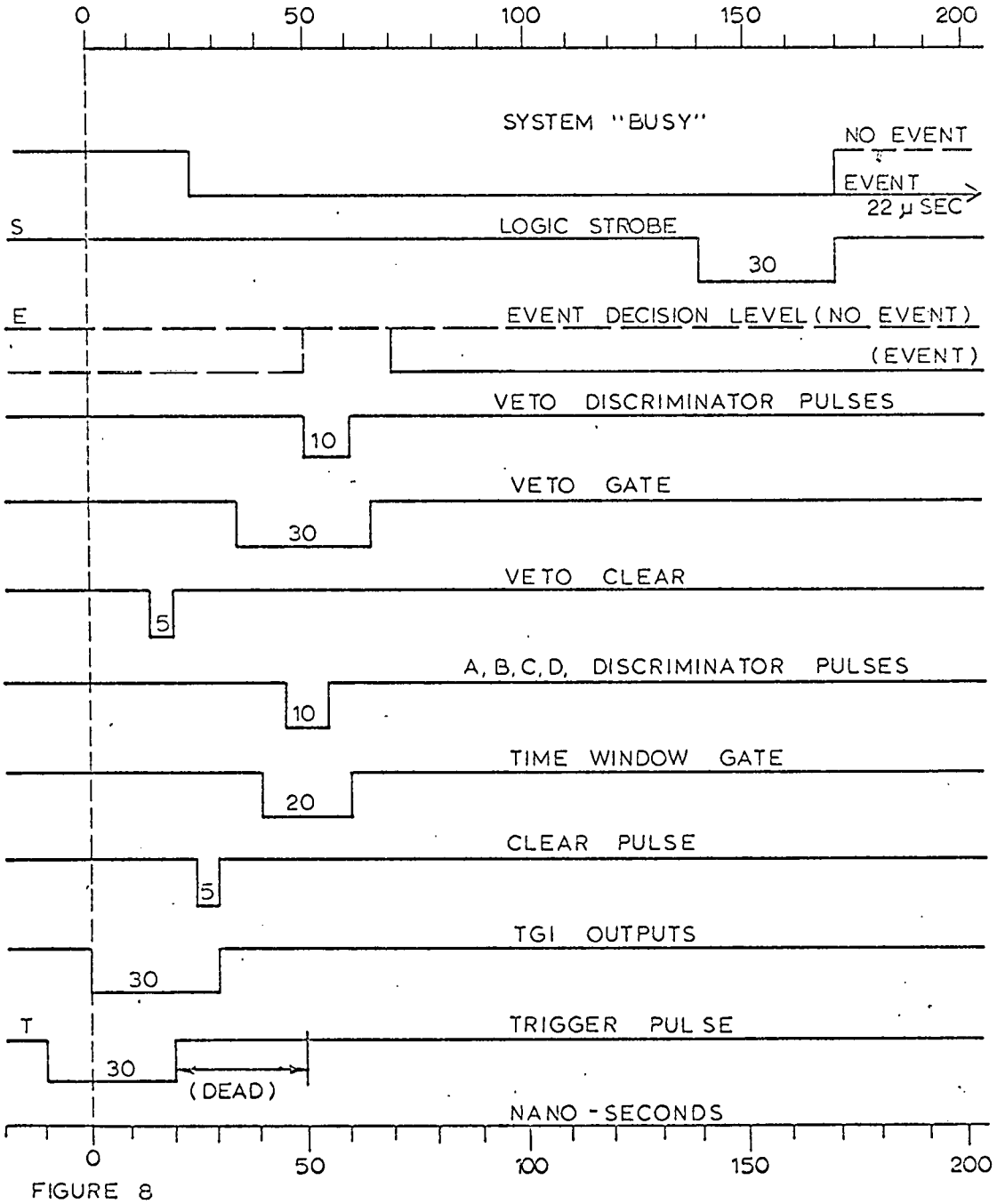

FIGURE 8
TIMING OF THE LOGIC SYSTEM

was exceeded, the data in the core were written on magnetic tape as one physical record with an IBM 729 IV transport. The format of this record is discussed below.

The data handler communicated the same information to a PDP-6 digital computer via its data control unit. In this way, on-line examination of the data could be performed to be assured the experiment was operating correctly.

E. Timing of the Counters

The hodoscope counters were timed by requiring a maximum coincidence rate with V_7. The technique was to set the timing so that the coincidence rate for charged particles through V_7 and each hodoscope element was a maximum. It was found that differences of 2 ns. were clearly observable in the rate. After the hodoscopes were timed, the Čerenkov detector was timed. Each of the individual tubes in the detector were timed. This was done by triggering a dual beam scope on $(D_8)\cdot(B_5)\cdot(V_7)$. These counters were chosen because they form a straight line near the beam direction. (One beam displayed B_5 and the other the Čerenkov signal. In this way, one could visually adjust the timing of the Čerenkov pulse to be coincident.

The timing of the gamma counters was more difficult since the detectors were placed completely out of the beam. Consequently, a totally different technique was used for timing. First, the

anticoincidence inner detector was disconnected and the CT·1γ (See pg.34) rate was measured as a function of gamma timing. The timing that gave the maximum rate was taken as correct for the outer half of the gamma counter. Then, the anticoincidence half of the gamma counter was installed into the circuitry. The CT·1γ rate was then minimized by adjusting the timing of the inner half.

F. Data Taking Technique

The data taking technique was intentionally redundant in order to make checks to guard against machine errors in writing the tape and human errors during the experiment.

The experiment was performed with one magnet polarity (A polarity) for approximately 1/2 hour, and then with the other polarity (B polarity) for about 1/2 hour. Each time the magnet polarity was changed, a new run was begun. The run number was recorded on 4 ten position thumb switches which, via a diode matrix, was converted to binary coded decimal. The approximate magnet current in amperes was set in 4 of the thumb switches and the magnet status (0 = off 1 = A polarity 2 = B polarity) was set in 1 switch. The switches labelled A, B, C, ..., W, are shown in Figure 9. All 23 of these switches were recorded on tape as described below.

In order to check the data output device, all 4 bcd bits of O and P were set to one and all 4 of Q and R were set to zero.

A	B C D E F G H I J K L M N O P Q R S	T U V W
1	0 8 7 5 - - - - - - - - - - - - - - - -	1 0 6 3
Mag. Polarity	Magnet current	Run No.

Figure 9

Meaning of the Thumb Switches

During the course of each run, 15 scalers were counting. The meanings of the scalers are shown in Table 1. Here the term CT has been used to describe a complete trigger:

$$CT = (D_R=1)(D_L=1)(B_R=1)(B_L=1)(G\neq 0)(A=2)(\overline{\Sigma V})$$

and CAT is a complete trigger with angle logic included:

$$CAT = CT\cdot(\measuredangle_L)\cdot(\measuredangle_R).$$

Also, the run number, the magnet current as measured in millivolts across a shunt and magnet polarity as measured by a Hall-probe were recorded.

Scalers 8 and 9 were used as logical checks just as were thumb switches 0, P,Q and R. Since scaler 8 and switches 0 and P formed one 36 bit word, all BCD bits of scaler 8 were set to 1. Similarly, all bits of scaler 9 were set to 0. These could be used later for logical checks.

Since the apparatus consisted of 36 hodoscope counters, the configuration of the system of hodoscopes was described by a 36 bit binary word. This was particularly convenient for later analysis on a 36 bit Univac computer. The remainder of the data had to be packed into an integral number of 36 bit words. It was found that this could be done with only one more word which had to be packed

Scaler Number	Meaning
1	CT gamma = 0
2	CT gamma = 1
3	CT gamma $\geq$ 3
4	CAT gamma = 0
5	CAT gamma = 1
6	CAT gamma = 2
7	CAT gamma $\geq$ 3
8	See text
9	See text
10	CAT gamma = 0 $\breve{C} \geq 7$
11	CAT gamma = 2 $\breve{C} \geq 7$
12	G. 10 + 90 degrees rate
13	CL/1000
14	CR/1000
15	VO singles

Table 1

Meaning of the On-line Scalers

into an integral number of 36 bit words which contained pulse height information concerning the Čerenkov detector and the beam intensity as measured by the G 10 monitor. Also, it had to contain information about the 4 gamma counters, the veto counters, and finally logical tags used as checks on the validity of the event against errors in the recording electronics. The data was then stored in 2 words called WORD1 and WORD2. These are shown in Figure 10.

In WORD2, $\overline{G1}$ is the inner half of gamma counter 1 and G1 is the outer half of gamma counter 1. The beam intensity and Čerenkov pulse height were the 6 bit outputs of analog to digital converters. The remainder of the information is redundant since it is all contained in WORD1.

The format of the data written on tape is shown in Figure 11. Each record was made up of a 17 word preface as well as the data for each event. The run number, the thumb switches A through W, the on-line scalers and the magnet current were written in BCD. The scalers were 7 digits and the digital voltmeter output from the magnet was 5 digits.

The data were written on 7 track 556 b.p.i. on 2400 foot tapes. The end of each tape was marked with several ends of file.

Also associated with each run were 25 off-line scalers. These were employed for the purpose of checking for malfunctions of the

WORD1

A1	A2 ··· A16	B1 ··· B4	B5 ··· B8	D1 ··· D6	D7 ··· D12
	A	B left	B right	C left	C right

WORD2

$\bar{G}1\bar{G}2G1G2\bar{G}3\bar{G}4G3G4$	V1···V7	001010	100100	1	1	0	1	1	00	1	1
Gamma Counters	Veto Counters	Cerenkov Pulse Height	Beam Intensity	$A = 2$	$B_L \cdot B_R = 1$	$\Sigma V \geq 1$	$D_L = 1$	$D_R = 1$		$\gtrless R$	$\gtrless L$

Figure 10

Packing of the Data from Each Event

4 DIGIT BCD RUN NO.		12 BIT BINARY WORD COUNT
HALL PROBE POLARITY		MAGNET CURRENT - 5 BCD BITS
CLOCK TIME AND DATE		
		on line scaler 15 - 7 BCD Bits
		on line scaler 14
		on line scaler 13
W		on line scaler 12
U	V	on line scaler 11
S	T	on line scaler 10
Q	R	on line scaler 9
O	P	on line scaler 8
M	N	on line scaler 7
K	L	on line scaler 6
I	J	on line scaler 5
G	H	on line scaler 4
E	F	on line scaler 3
C	D	on line scaler 2
A	B	on line scaler 1

LAST EVENT - WORD2

LAST EVENT - WORD1

.

.

.

FIRST EVENT - WORD2

FIRST EVENT - WORD1

Figure 11

Packing of Each Block of Data

apparatus. These were printed out by an automatic typewriter when TGO reached a preset total. The scalers printed out were:

1	$\overline{TGI}$	
2	TGO	
3	$\gamma=1$	CT
4	$\gamma=2$	
5	$\gamma\geq 3$	
6	$\overline{\gamma=0}$	
7	$\gamma=1$	
8	$\gamma=2$	
9	$\gamma\geq 3$	(CAT)·(Čerenkov Pulse Height $\leq$ Channel 7)
10	$\gamma\geq 0$	
11	$\underline{\gamma=2}$	
12	V_7	singles
13	V_7	noise
14	$\overline{G1}$	
15	G1	
16	$\overline{G2}$	
17	G2	
18	$\overline{G3}$	
19	G3	
20	$\overline{G4}$	
21	G4	
22	ungated G 10 monitor	
23	gated G 10 monitor	

24 singles gates

25 noise gates.

These scalers were gated on and off by a digital clock, the predet. In this way, the V7 (first veto) count rate during the spill and also the noise rate (between beam spills) were measured on scalers 12 and 13. Scaler 12 was gated by the spill gate and scaler 13 was gated by a 100 msec. pulse from the predet during the time when the beam was off. These scaler outputs were used as a check of both the operation of the apparatus and also of the AGS. For example, it was found that (V7 singles)/(G 10 monitor) was constant until the G 10 target went bad. This is reasonable since V7 was located at -20° and the G 10 monitor at $+90^{\circ}$. When the target curled up because of heating, an unusual angular distribution resulted causing V_7/G 10 to change.

IV. DATA ANALYSIS

A. Central Idea

The best possible way to look for a CP violation in the data from $K_{3\pi}$ would be to make a Dalitz Plot of the background subtracted data. A CP violation would show up as an asymmetry between the left and right sides of the plot. To make such a plot, it is necessary to know the kinetic energies of the π^+ and π^- in the rest frame of the K_L^o. Unfortunately, it is not possible to transform the data to the rest frame because the momentum of the incident K_L^o is unknown and also, there is virtually no information available concerning the π^o. For these reasons, the horizontal transverse components of the π^+ and π^- momenta (hereafter called transverse momentum) were studied. They are unchanged by a transformation between the laboratory frame and the center of mass frame. The transverse momentum distribution for the π^+ and π^- were compared. Any statistical significant difference between the two spectra could imply a violation of CP.

In order to relate such a difference to a physical parameter such as $\sigma_{\pm}$ from the linear approximation to the matrix element

$$\frac{\rho}{\phi} = 1 + 2\sigma_o(2T_o - T_{max})\frac{M_K}{M_{\pi 2}} + 2\sigma_{\pm}(T_+ - T_-)\frac{M_K}{M_{\pi^2}}$$

it was necessary to find what asymmetry in the momentum spectrum was implied by a given value of $\sigma_{\pm}$. Here ρ is the density of events in the Dalitz plot ϕ is the density of phase space. To do this, a large number of physical distributions had to be folded together.

Included in these were the geometrical efficiency of the detectors, the quantum efficiency of the detectors and the incident K_L^o beam characteristics. To do this analytically would be an extremely difficult if not impossible task. For this reason, a Monte Carlo simulation program was written with σ_0 and $\sigma_\pm$ as fitting parameters. A chi squared program was used to determine the values of $\sigma_\pm$ and σ_0 for the best fit of the Monte Carlo to experimental data.

B. The Monte Carlo Program

The Monte Carlo program was run as a two part process. First the momentum vectors in the lab system of the π^+, the π^-, and the 2 gamma rays from the π^o decay were generated and stored on tape. One tape was generated for decays consistent with a constant matrix element, a CP violating matrix element and a CP conserving matrix element. The linear approximation to the matrix element was employed as described above. The program used to generate the decays, or explosions was called EXPGEN.

Second, these decays were distributed through the decay region of the apparatus and were allowed to pass through the appratus to be detected. The decay of the π-meson to a muon was accounted for. This program was called APEXP. It generated data tapes in a similar format to the experimental tapes.

C. Monte Carlo Program Part I - EXPGEN

The first half of the Monte Carlo program contained kinematical transformations and quantum mechanics associated with the decay. The standard Monte Carlo techniques were used. Parameters were "chosen consistent with some distribution". That means, a value E of the parameter was chosen at random. If Prob (E) was greater than or equal to a number, R chosen at random, the value E was accepted. If not, a new value of the parameter was chosen and another try was made, and so on.

The mechanics of the program were straightforward. The value of the incident K-meson momentum was chosen consistent with the AGS beam spectrum. The form of the spectrum used was

$$\text{Prob}\ (p) = p/p_o e^{-p/2p_o}$$

$$p_o = 0.28\ \text{BeV/c}$$

$$1\ \text{BeV/c} \leq p$$

This was first used by Bennett et al. It is consistent with the spectra obtained by many experiments performed in the K_o beam.[30]

The total mass of the $\pi^+ + \pi^-$ system, $M_{2\pi}$, was chosen consistent with the phase space distribution. The system was treated

as a 2 particle decay in which the K-meson decayed to a π° and an aggregate $\pi^+ + \pi^-$ particle. The phase space associated with the decay is given by:[31]

$$\phi(M_{2\pi})dM_{2\pi} = \sqrt{(M_{2\pi}^2 - 4M_{\pi\pm}^2)(M_{2\pi}^2 + (M_K^2 - M_{\pi^\circ}^2)^2) - 2(M_K^2 + M_{\pi^\circ}^2)M_{2\pi}^2}\; dM_{2\pi}$$

This is the product of the two phase space relations for the decays

$$K_L^\circ \rightarrow \pi^\circ + (2\pi)$$

$$(2\pi) \rightarrow \pi^+ + \pi^-.$$

A value of the quantity $M_{2\pi}$ was chosen. Then, a random direction for the π^+ was chosen in the $M_{2\pi}$ rest frame and the opposite direction is assigned to the π^-. The two particles were Lorentz transformed to the K_L° rest frame. In this way, a 3 particle decay was generated consistent with a phase space distribution for the momenta of π^+, π^- and π° in the K_L° rest frame.

The results of this subprogram then had a matrix element folded in. The 3 matrix elements used were

$$M = 1$$

a constant,

$$M^2 = 1 + \frac{2}{3}(T_{\pi^+} - T_{\pi^-})\frac{M_K}{M^2_{\pi\pm}} = 1 + \frac{x}{3}$$

a CP violating matrix element with $\sigma_{\pm} = \frac{1}{3}$, and

$$M^2 = 1 + \frac{2}{3}(2T_{\pi^o} - T_{max})\frac{M_K}{M_{\pi^\pm}} = 1 + \frac{y}{3}$$

a CP conserving matrix element with $\sigma_o = \frac{1}{3}$.

If the event was accepted as consistent with the matrix element histogramming of the kinetic energies of the π^+, the π^- and their sum and the incident K^o momentum was performed.

The acceptable event was then transformed to the laboratory. The direction cosines of the π^o were randomly chosen and the cosines of the π^+ and π^- were rotated through these angles and the energy and momentum of the 3 π-mesons were Lorentz transformed to the laboratory frame.

The decay of the π^o was then allowed to occur. Since the decay takes place within 10^{-5} cm., the π^o is taken to decay at the same place as the K^o decay. The gamma rays are each given an energy of half the rest mass of the π^o (67.4875 MeV) in the rest frame of the π^o. The gamma rays were assigned random opposite directions, and then Lorentz transformed to the lab frame. The two gamma rays were rotated through the angles associated with direction cosines of the π^o in the lab frame.

The events generated were written on magnetic tape for analysis later.

D. Monte Carlo Program Part II - APEXP

The second half of the Monte Carlo program was used to geometrically detect the decays generated by EXPGEN. The decay of the π-mesons:

$$\pi^{\pm} \rightarrow \mu^{\pm} + \bar{\nu}.$$

was included. The spaces between the counters were ignored.

The decays read into the program were plotted in a Dalitz Plot in order to be sure EXPGEN was generating meaningful data. Specifically, the Dalitz Plot of the data for a constant matrix element was examined and found to be uniform. The Dalitz plots for matrix elements of 1, $1 + x/3$ and $1 + y/3$ are shown in Figures 12, 13, 14, respectively.

Each decay was assigned decay points in the decay region (between the A hodoscope and V_7). The decay position was chosen consistent with the lifetime:

$$c\tau_K = 1593 \text{ cm.}^{32}$$

The relativistic time dilation was accounted for. The coordinates of the decay point transverse to the beam were chosen consistent with a beam distribution similar to the actual one. The actual distribution of neutrons in the beam was measured using a neutron telescope. The counting rate in this telescope versus position is

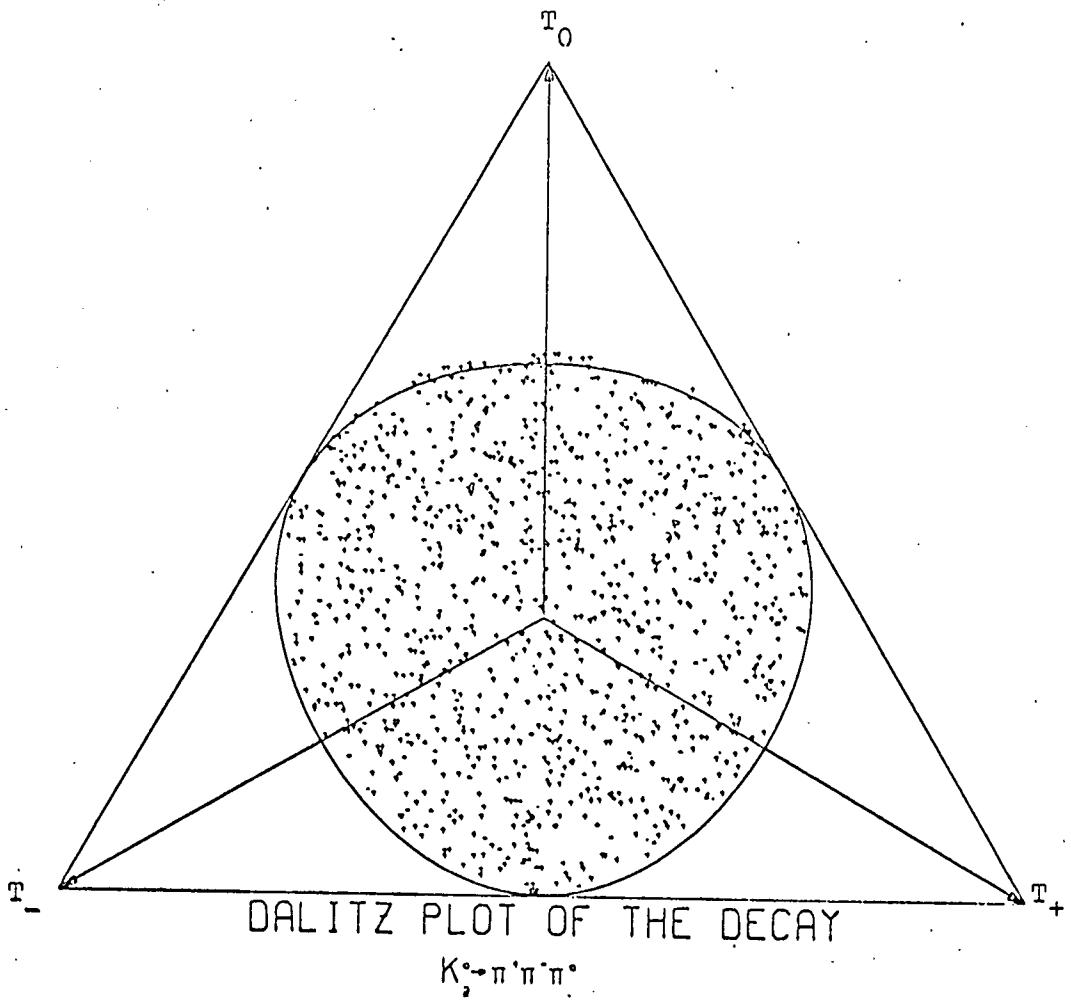

Figure 12

Dalitz Plot of Monte Carlo Data

for a Constant Matrix Element (1)

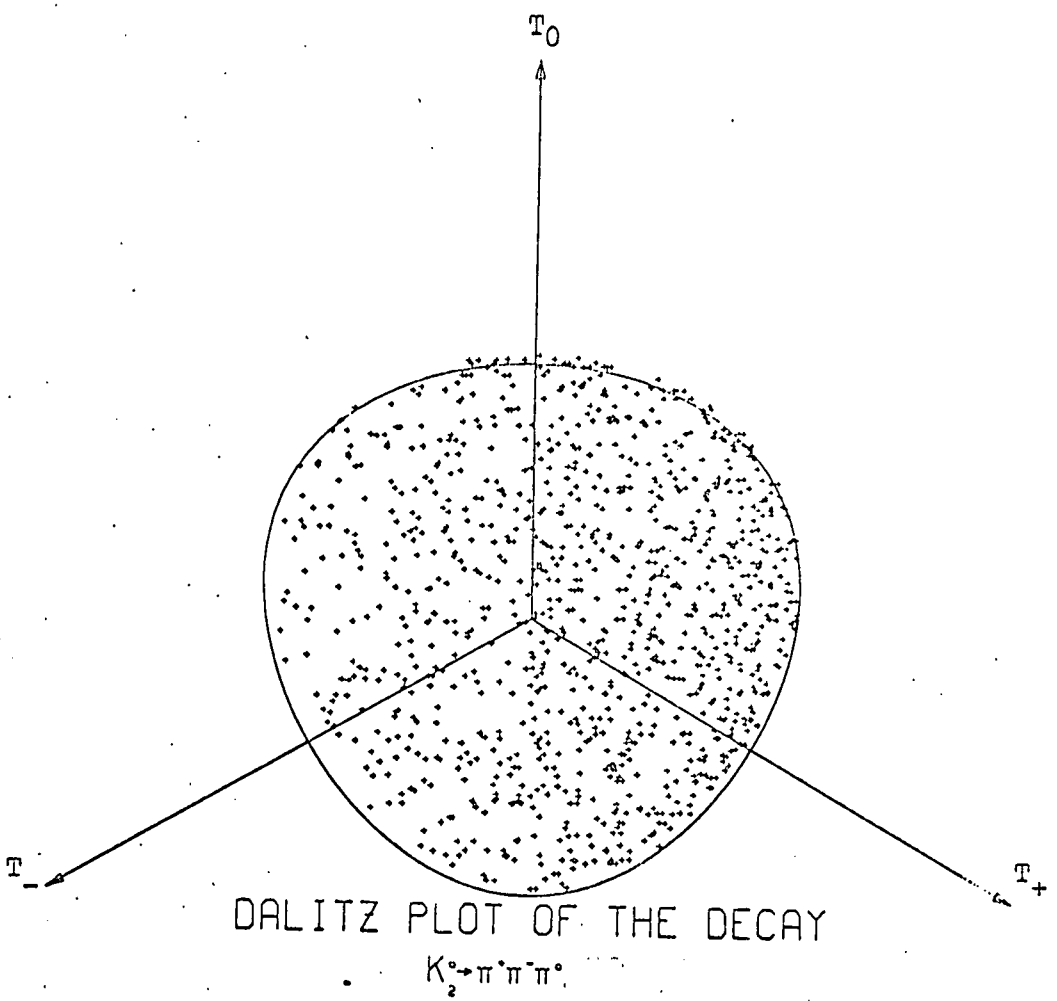

Figure 13

Dalitz Plot of Monte Carlo Data for a

CP Violating Matrix Element $(1 + \frac{x}{3})$

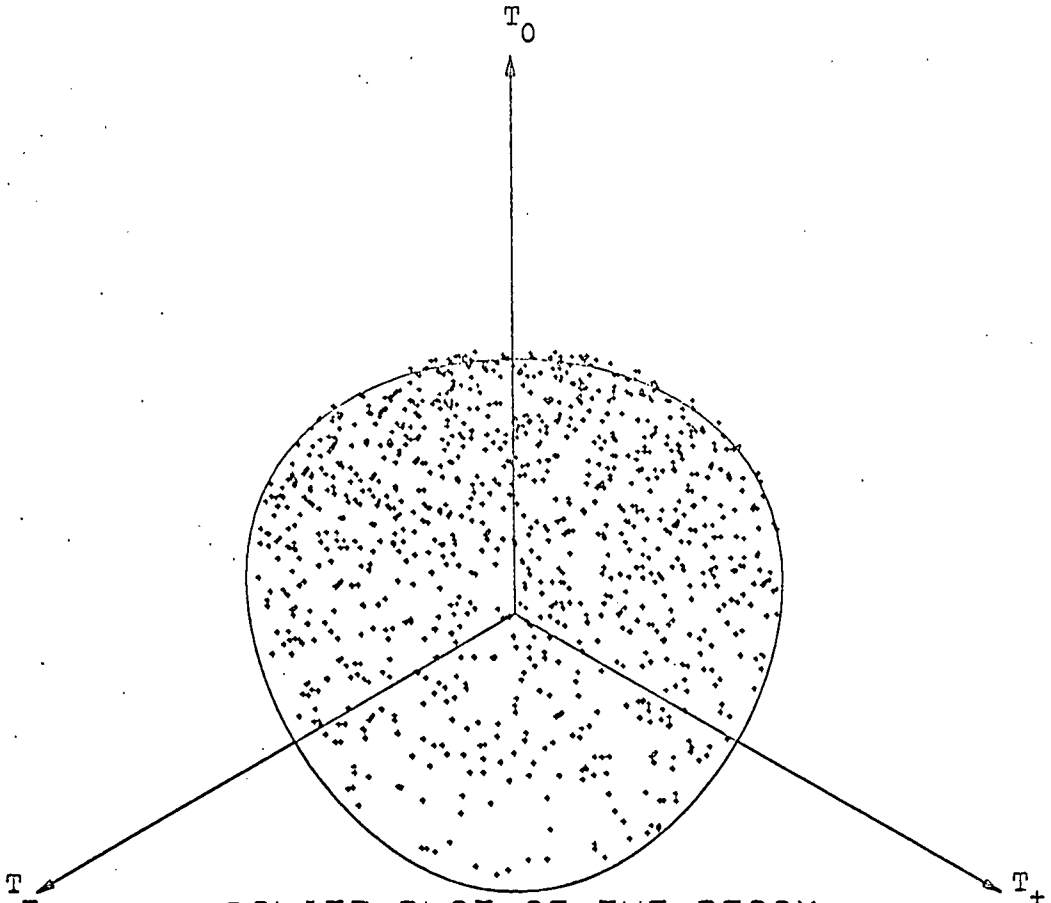

Figure 14

Dalitz Plot of Monte Carlo Data for a

CP Conserving Matrix Element $(1 + \frac{y}{3})$

shown in Figure 15. The curve is not symmetric due to the finite size of the target. The length of the target is not perpendicular to the beam direction. Rather, it appears at 70 degrees. In the actual running of the experiment, this asymmetry was of no consequence because the experiment was performed using both magnet polarities and later averaged. In this way, the beam asymmetry was averaged out. In the Monte Carlo calculation, this polarity averaging was not performed. Instead, symmetrized beam distribution was used. This distribution is also shown in Figure 15.

The form used was created by taking linear sides whose slope was the average of the real slopes. The center of the model distribution was peaked by linear approximations to the actual distribution. No measurement was taken of the vertical distribution but it was certainly symmetric since the geometry in the vertical direction was symmetric. For this reason, the same symmetric form was taken in this direction.

The two charged π-mesons were allowed to evolve in time, traversing each of the hodoscopes. The counters were assumed to be 100 percent efficient. (They were more than 99% efficient.) As the particles traveled through the apparatus, they were allowed the possibility of decaying to muons. It was found that in approximately 20% of the events the π's decayed.

The charged particles were passed through the magnet by using the effective length approximation. The impulse delivered to a particle for various paths was calculated. This is shown in Table

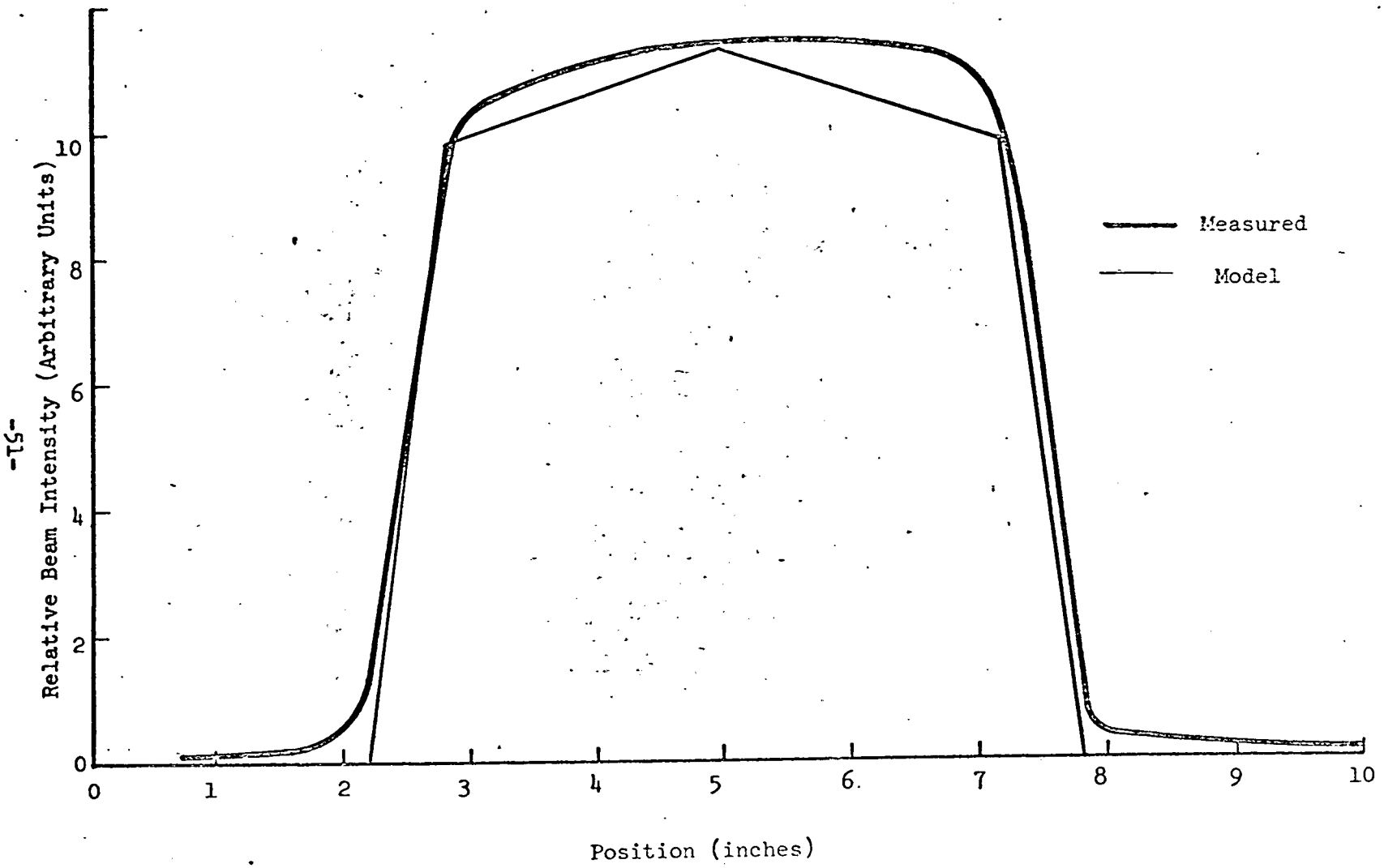

Figure 15 Beam Profile

2. The maximum variation is 6 percent.

A charged particle's track was accepted if it passed through all 3 hodoscopes and the magnet aperture. No angle logic requirement was used. This was reasonable since analysis showed 90 percent of the events generated satisfied angle logic.

The subprogram for the detection of the gamma rays was not as straightforward. The detection efficiency of the gamma rays was not sufficiently large to be treated as 1. The detection of the gamma ray had to be dealt with as a 2 part process. First, did the gamma ray convert in the lead and second, did the charged particles from the gamma conversion make it out of the lead and into the scintillator. The first stage of the process was performed using linear approximations to the pair production cross section.[33] The approximation is shown in Figure 16. Handling of the 2 charged particles from the pair production was facilititated using charged particle Monte Carlo shower calculations.[34] The calculation tabulates the probability of no particles of energy at least E for an incident electron of energy E_o having traversed a thickness of R radiation lengths of material. For this calculation E was taken to be 5 MeV, perhaps a bit high for 1/4 inch scintillator but it was found that the probabilities were very nearly the same at energies within a factor of 2, so the more complete information available at 5 MeV was used. The thickness used was

Trajectory Coordinates		Impulse Delivered ΔP(MeV/c)	(Magnet Current at 1850 amps)
Vert.	Hor.		
$7\frac{5}{16}$"	- 11.5"	142.07	
$-7\frac{5}{16}$	- 11.5"	138.40	
$7\frac{5}{16}$	0	142.40	
$-7\frac{5}{16}$	23.0	133.0	

Table 2

Impulse Delivered by

Analyzing Magnet

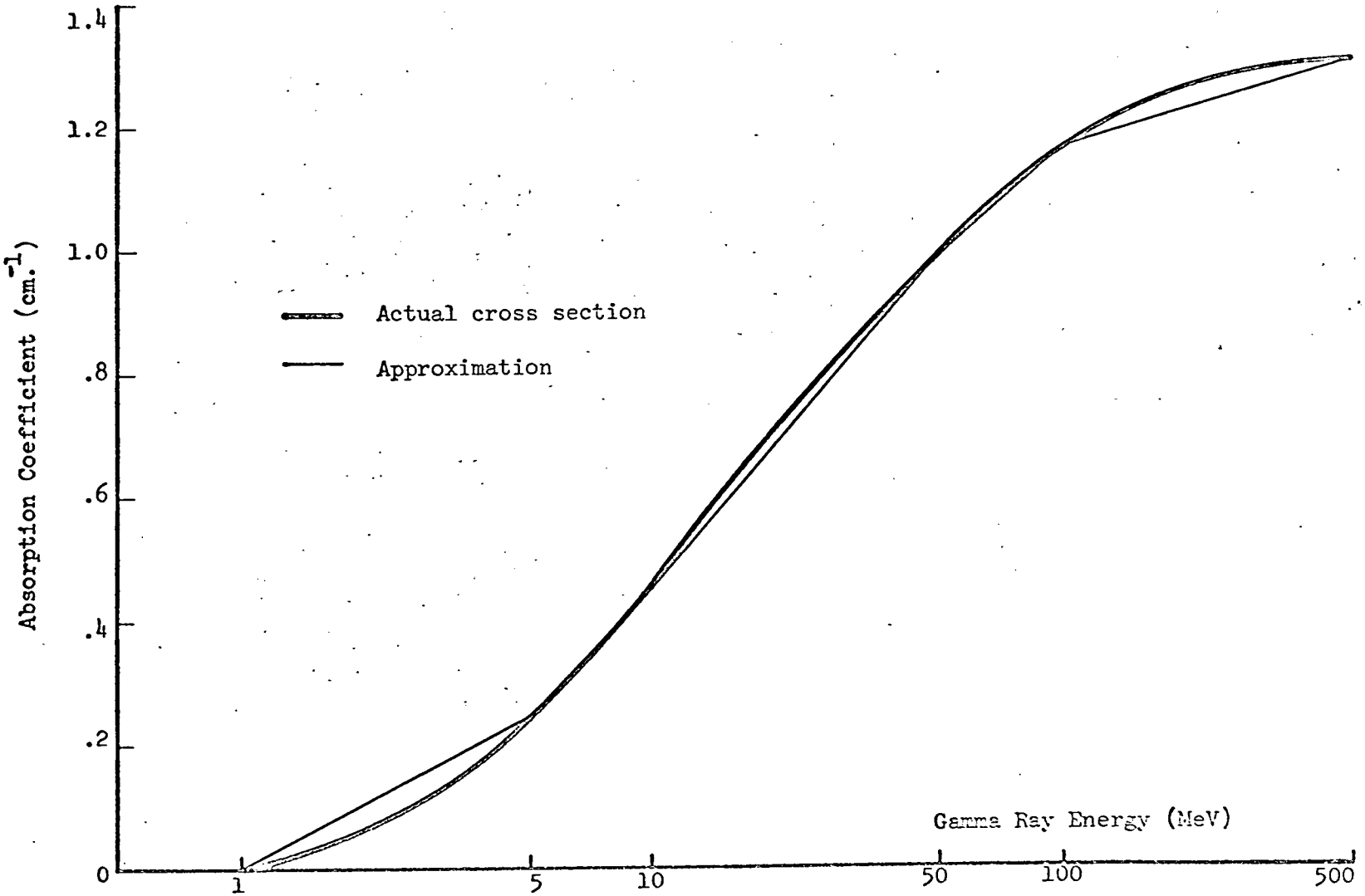

Figure 16 Approximation to Pair Production Cross Section

$$R = 1/\cos\theta - L \text{ radiation lengths}$$

where θ is the angle to the normal of incident gamma and L is the distance in radiation lengths the gamma traveled before pair producing. This technique was suitably accurate as indicated by the agreement of the ratio of 1γ to 2γ events between Monte Carlo result and experiment. The experimental ratio was 10.8 and the Monte Carlo result was 11.2. If the efficiency of the gamma counters is assumed to be 100%, the ratio is only 6.

E. Analysis of Hodoscope System

The finite width of the hodoscope elements used in this experiment limited the precision of the reconstruction of an event. This phenomenon is of particular importance for reconstruction of momenta. Knowledge of the uncertainties of momentum measurements leads to intelligent binning and cutting of experimental data.

A program was run on the Case Western Reserve University high energy physics IBM 1800 computer to examine the uncertainties of the reconstructed transverse momentum for all possible counter combinations. The program converted counter numbers to real space coordinates. It ignored the space between counters. The coordinates associated with the counters triggered were used to calculate the horizontal projection of the momentum vectors of both tracks PL and PR.

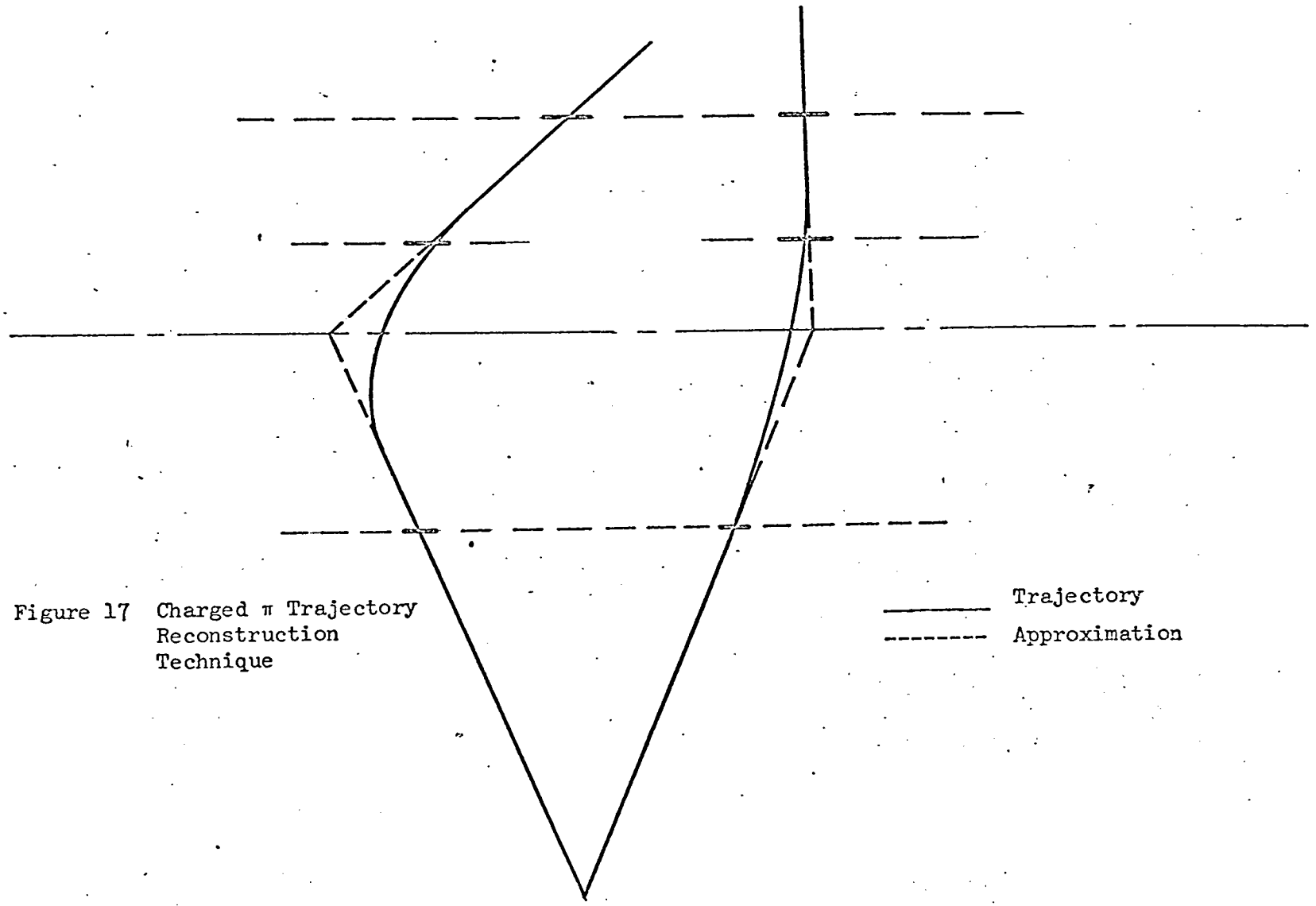

Figure 17 Charged π Trajectory Reconstruction Technique

The geometrical reconstruction was performed using an impulse approximation for the effect of the magnetic field. The magnet was assumed to have delivered momentum to each of the charged particles when they were half way through the magnet. The value of the impulse used in the program was

$$\Delta p = \pm 0.077 \; I \; \text{MeV/c}$$

where I was the magnet current in amps.

The geometrical reconstruction technique used is shown in Figure 17. The counters that had fired have been indicated by darkening them in.

This reconstruction program was written for analysis of the experimental data but was also used in this calculation. In this case, non-integral counter numbers were considered. If counter number A4 was turned on, the program would consider a trajectory passing through the center of A4. If A4.3 was assumed to be turned on, the trajectory considered would pass three tenths of an A counter width to the left of A4's center. In this way, the edges rather than the center of each counter could be considered by using half integral numbers.

In order to get an idea of the uncertainties in the various measurements, an integration of trajectories was to be performed over the width of the counters. For any counter, n, the trajec-

tories were to be considered over the range counter number $n - 1/2$ to counter number $n + 1/2$.

The program was written to consider finite segments of the counters and perform the integration. Because the total number of counter combinations was large, any program for examining all counter combinations would have been very time consuming. For this reason, only 2 positions were considered for each counter - the edges.

For each counter combination, the 8 trajectories through the edges of the A, B, and D counters were considered. Eight values of transverse momentum were calculated and compared to the "central value" or the transverse momentum of a particle whose trajectory passed through the centers of the 3 counters. The root mean squared deviation from the "central value" was calculated for those values greater than the "central value" $(\Delta p_\perp^+)$ and for those less $(\Delta p_\perp^-)$.

The results of this program show that the uncertainties vary tremendously and also that the reconstructed data sometimes was unphysical - that is, negative values of $p_\perp$ occurred occasionally.

Using a representative 6000 events, the frequency of each counter combination was obtained. Using this information, it was possible to determine what percent of the data remained if various requirements were placed on the reconstruction. The re-

Restriction	% of Data Remaining
reconstructed momentum is positive ($p_{\parallel}^{c} > 0$)	98%
$p_{\perp}^{c} > 0$ & $\Delta p_{\parallel} \leq 100\%$	69 %
$p_{\perp}^{c} > 0$ & $\Delta p_{\parallel} \leq 90\%$	66 %
$p_{\perp}^{c} > 0$ & $\Delta p_{\parallel} \leq 80\%$	62.4%
$p_{\perp}^{c} > 0$ & $\Delta p_{\parallel} \leq 70\%$	62 %
$p_{\perp}^{c} > 0$ & $\Delta p_{\parallel} \leq 60\%$	52 %
$p_{\perp}^{c} > 0$ & $\Delta p_{\parallel} \leq 50\%$	46 %
$p_{\perp}^{c} > 0$ & $\Delta p_{\parallel} \leq 40\%$	38 %
$p_{\perp}^{c} > 0$ & $\Delta p_{\parallel} \leq 30\%$	24 %
$p_{\perp}^{c} > 0$ & $\Delta p_{\parallel} \leq 20\%$	12 %
$p_{\perp}^{c} > 0$ & $\Delta p_{\parallel} \leq 10\%$	1.6%
$p_{\perp}^{c} > 0$ & $\Delta p_{\parallel} \leq 5\%$	0 %

Table 3

Possible Cuts on Data and Amount of Data Lost

A	B	D
1	2	2
1	3	3
1	3	4
1	4	4
1	4	6
2	2	2
2	3	3
2	3	4
2	4	4
3	2	2
3	3	3
3	3	4
3	4	4
4	2	2
4	3	4
4	4	4
6	3	3
7	3	3
7	4	5
8	3	3
8	4	4
8	4	5
9	3	3
9	4	4
9	4	5
10	3	3
10	4	5
12	4	4
13	4	4
14	4	4
15	4	4

Table 4

"Bad" Counter Combinations

sult of such studies is given in Table 3.

It can be seen that the cut $p_{\perp}^{c} > 0$ and $\Delta p_{\perp}^{\pm} \leq 70\%$ (here c refers to "central value") is worth investigating because the resolution of the hodoscope system is dramatically increased in exchange for a reasonable loss of data. Any more stringent requirement on the data would greatly reduce the number of events to be considered. The counter combinations associated with this cut are given in Table 4. The events satisfying this constraint will henceforth be referred to as good and those not, as bad.

F. Experimental Data Reduction Program - TANAL VI

The computer program for reading the experimental data tapes was intricate because of all the decoding and checking that had to be done. The construction of the program was built of many subprograms written in Sleuth II assembler language, Algol 60 and Fortran V compiler languages. The actual program to read the tape was written in Sleuth II by the Case computing center staff. This subprogram KENTAPE was written in the assembler language because the compiler language could only read tape written in a specific format containing a fixed number of words per record. Also, since the tape contained parity errors due to hardware failures during the writing, the program had to be able to read this tape, recognize the problem and set an error flag. Since

this Sleuth program was used, the main program and some subprograms had to be written in Algol 60 because Fortran V cannot use external subprograms in any language other than Fortran. The programs which did not need the advantages of Algol were written in Fortran. Although Algol is a highly sophisticated compiler, it is also a very inefficient language time-wise since a program written in Algol will run 3 to 5 times slower than one written in Fortran.

The program sorted out blocks of data containing parity errors and ignored them. It decoded the run number of each block and decided whether to bin the data, skip the block or print out the results to that point. The final print out was caused by exhaustion of runs to be analyzed or by encountering an end of file.

For each block to be analyzed, a series of checks were performed on the preface of the data block. The magnet current as measured on the digital voltmeter across the magnet windings was compared to the thumb switches for 5% agreement. The magnet polarity as measured by a Hall probe in the magnet was compared to thumb switch A. The sum of the run number plus the value of thumb switch was checked for oddness.

If any of these conditions was not met, an error message was printed and another block read. A check was made on the magnet current. If this had varied from the value in the previous block

by more than 0.1 percent an error message was printed and another block read.

The values of each of the 15 on-line scalers were decoded and running totals were kept on each of them. When a data block passed the above requirements, control was returned to the main program. Then WORD2 was decoded for each event. If all of the logical checks in WORD2 were successful and no vetoes were on, WORD1 was decoded. The event was then binned as described below.

Because of the high cost of computer time, the analysis program had to make only one pass to bin all of the data. For that reason, the number of quantities binned is quite large. There were two types of binning performed. First, the actual counter combinations (which elements of each hodoscope fired for both left and right tracks) were binned for all relevant cases and second, data which could not be reconstructed from the counter combination tables was histogrammed for all relevant cases.

The histograms were each 100 bins plus overflow and underflow. The quantities histogrammed were $\Delta p = p_{\perp \text{ left}} - p_{\perp \text{ right}}$, x (transverse decay coordinate) and z (longitudinal decay coordinate). There were 40 histograms in all for the cases $\gamma = 0, 1, 2$ for clean and dirty and $\breve{C} \leq 7$ and $\breve{C} > 7$. A dirty event is defined as one for which one or more extra inner or veto gamma counter half was "on" during the event. The $\breve{C}$erenkov requirement of a pulse height of less than channel number 8 corresponds to no electron passing through the $\breve{C}$erenkov veto. This can be seen from

Figure 18. The electron peak can clearly be seen and the $K3\pi$ contribution can also be seen (note the split vertical scale). Using the cut off in channel 7 yields essentially no loss of $K3\pi$ events and a Ke3 contamination of less than 1%.

There were 14 pairs (left track and right track) of counter combination tables. The cases 0γ, 1 and 2γ clean and dirty for $\check{C} \leq 7$ and $\breve{C} > 7$ were binned. Also the case of extra counters on was considered. If only one of 2 tracks had extra hodoscope elements on, the other set of counter numbers was binned for 0γ, 1 and 2γ. Finally, the counter combinations for 2γ events with opposite gamma counters were binned.

The advantage of binning counter combination tables rather than histograms of reconstructed pion momenta is that more information is retained. Using the tables, various cuts could be made on the data and then extract momentum histograms. This could be done without rereading all of the data tapes any number of times.

It should be noted that decay coordinates and $\Delta p = \vec{p}_{left} - \vec{p}_{right}$ cannot be reconstructed from single track counter combinations so these quantities had to be binned directly in as many cases as possible.

Typical Pulse Height Spectrum
for Electron Discriminating
Cerenkov Detector

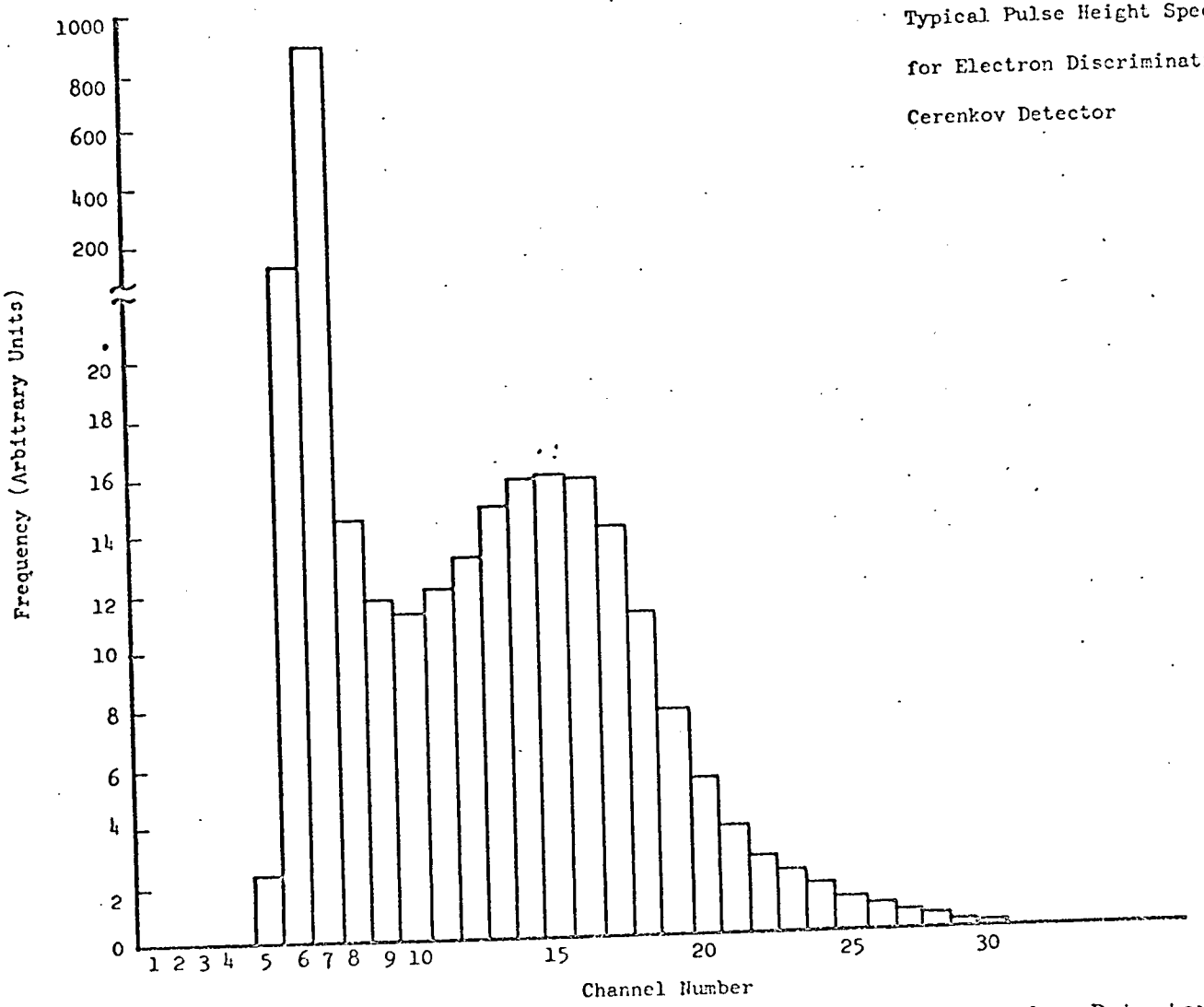

Figure 18 Pulse Height Spectrum for Cerenkov Detector

G. Reduction of Experimental Data

The experimental data tapes were read and binned by Tanal VI. If the parameters of several (up to 10) runs were the same (beam intensity, magnet current, gas in decay regions, etc.), the runs were binned together.

In addition to printing the results on paper, the data were punched on cards. The cards were subsequently read by the IBM 1800 computer and copied onto magnetic tape in BCD format. The IBM format was used because it is compatible with SDS format so that the data could be treated on the Harvard University High Energy Physics Sigma 7 computer.

The raw histograms and tables on the BCD tapes had to be corrected for chance gamma counts. The rate of 1γ events with a chance γ trigger (written as $1\gamma + (\gamma)$ was typically 15% of the 2γ rate and the $0\gamma + (\gamma)$ was 20% of the 1γ rate. These values were measured using delayed gamma counters. The precise amount of contamination depended upon the beam intensity. Specifically, the chance rate was proportional to the square of the beam intensity. This can be seen by realizing that the $n\gamma (n = 1, 2)$ chance contamination was proportional to the product of the gamma counter singles rate and the $(n-1)\gamma$ rate, each of which was proportional to the beam intensity. The percentage of contamination, however, was linearly proportional to the beam intensity. The data were chance corrected by subtracting the appropriate percent of 0γ

events from the 1γ and the 1γ from the 2γ. The background subtraction percentages used were

$$P_{0\gamma} = (20\%)\ G\ 10/6.46$$

$$P_{1\gamma} = (15\%)\ G\ 10/6.63.$$

Here $P_{0\gamma}$ and $P_{1\gamma}$ are the percentages of 0γ and 1γ events subtracted from the 1γ and 2γ data respectively, and G 10 is the average value of the G 10 monitor (via analog to digital converter so the value could be 0 to 63 units) during the data set under consideration. The chance corrected date were then added together to form complete chance corrected data sets for both A and B polarity for the cases of He and SF_6 in the decay region.

The chance corrected data werethen normalized so that the sum of all bins was unity. In this way, the various histograms could be compared directly independent of the number of events obtained in each mode.

In order to avoid introducing the bias of any geometrical asymmetry of the apparatus,the data were treated as if two experiments had been run simultaneously; one on the left side and one on the right side.

Treating both sides independently,the transverse momentum spectra for both magnet polarities were subtracted to obtain transverse momentum difference spectra. The magnitude of the asymmetry

for each was determined and the results averaged. In this way geometrical bias did not affect the results.

H. Fitting Monte Carlo to Experimental Data

The Monte Carlo transverse momentum asymmetry spectra had to be fit to the experimental data for four cases: 1γ and 2γ for all data (good + bad), and for the cut described in section IV G (good). Decays other than $K_{3\pi}$ could contribute appreciably to the 0γ data, so no fit was performed here.

The Monte Carlo program generated data using $\sigma\pm = 1/3$ (see Chapter II). This is the largest value of that parameter which maintains positive probabilities. Using the largest possible value of $\sigma\pm$ gives maximal $\pi^+\pi^-$ asymmetry, and thus good statistics can be obtained with minimum time. Monte Carlo transverse momentum spectrum for a smaller value of $\sigma\pm$ can be obtained by scaling down the $\sigma\pm = 1/3$ spectrum linearly with $\sigma\pm$.

Figure 19 is a histogram of the transverse momentum asymmetry spectrum for 1γ (good + bad). Superimposed is the Monte Carlo spectrum for $\sigma\pm = .003$. The Monte Carlo asymmetry is clearly visible. No such asymmetry can be seen in the experimental data. The data for incident K° momentum less than 2 GeV/c were considered separately. No variation in the asymmetry spectrum was found for any of the above four cases. A cut was also tried for longitudinal decay coordinate, z, less than 50 inches (physically, $0" \leq z \leq 72"$). This also did not affect the asymmetry spectra.

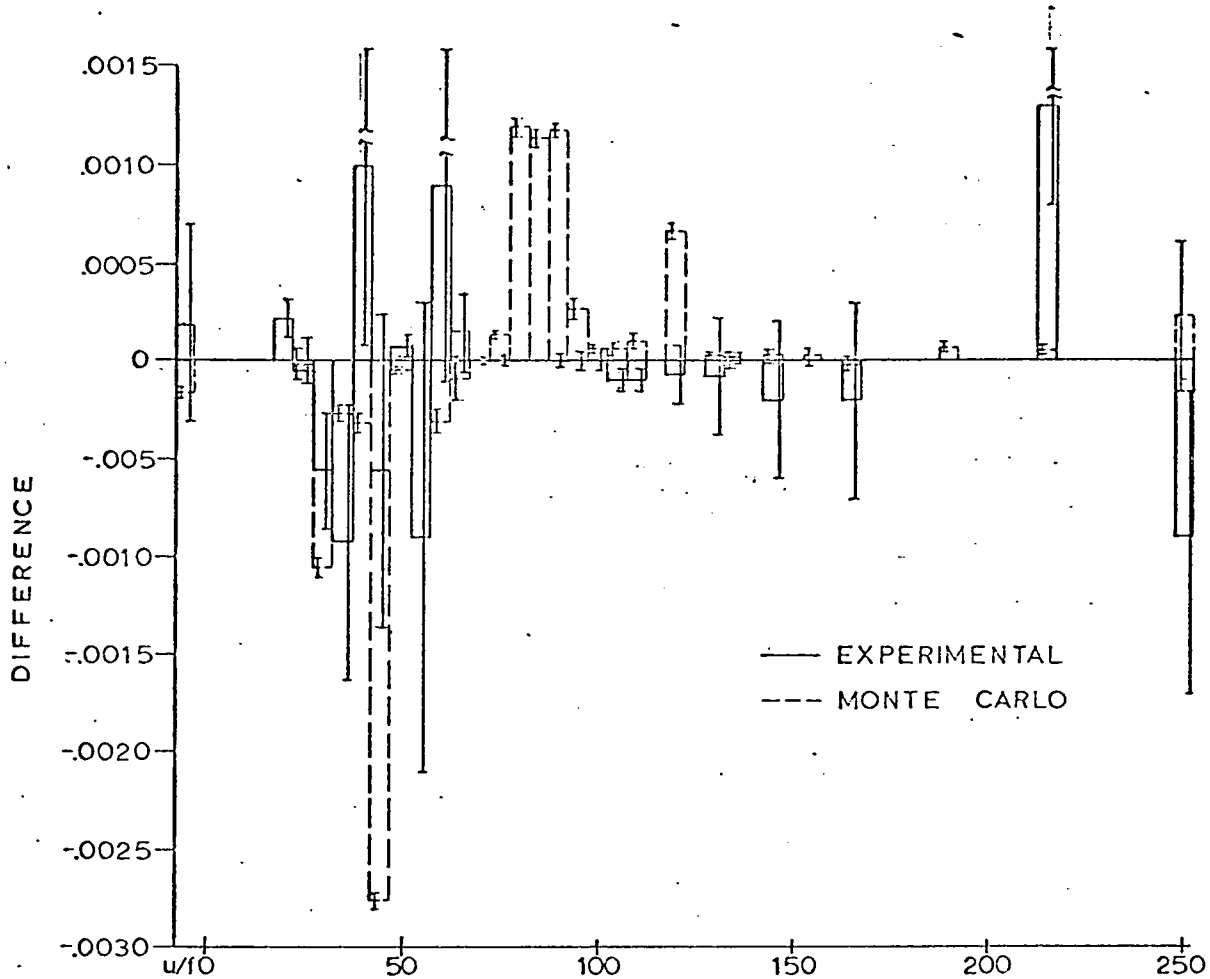

FIGURE 19
TRANSVERSE MOMENTUM ASYMMETRY SPECTRUM 1 δ (GOOD + BAD)

The Monte Carlo data were fit to the experimental using $\sigma\pm$ as the fitting parameter. The technique used was a chi squared fit. The value of $\sigma\pm$ was found which minimized the value of

$$\chi^2 = \sum_N \frac{(D_N^E - D_N(\sigma\pm))^2}{\sigma_N^2}$$

Here D_N^E is the N^{th} element of the experimental transverse momentum asymmetry spectrum, $D_N(\sigma\pm)$ is the N^{th} element of the Monte Carlo spectrum with CP violating parameter value $\sigma\pm$, and σ is $\sqrt{(\sigma D_N^E)^2 + (\sigma D_N)^2}$.

Figures 20, 21, 22, and 23 are plots of chi squared as a function of $\sigma\pm$ for 1γ (good + bad), 1γ (good), 2γ (good + bad), and 2γ (good). Each figure shows two curves; one associated with data from the left, the other representing data from the right. No geometrical asymmetry is visible from these data. The best averaged fits for the cases are for $\sigma\pm$ values of $-.0007 \pm .0009$, $.0001 \pm .0005$, $.0025 \pm .008$, and $.005 \pm .006$ respectively.

As a check on the fitting technique, the data were also used to obtain the parameter σ_o (see Chapter II). Rather than fitting the Monte Carlo transverse momentum asymmetry spectra to experimental spectra, the average of the π^+ and π^- spectra was used and a chi squared fit was made, similar to the asymmetry fit, only with σ_o as the fitting parameter. The case of 1γ (good + bad)

was fit yielding $\sigma_o = -0.20 \pm 0.05$. (See page 81).

The Monte Carlo predictions for the decay coordinate spectra, x (horizontal transverse) and z (longitudinal) were found to be the same for each matrix element assumed. The Monte Carlo x spectra predicted the experimental spectra quite well in that the acceptance of the apparatus was a constant over the region of the incident K^o beam.

The z spectra bear more consideration. Figures 24 and 25 are z spectra of 1γ and 2γ data respectively. The Monte Carlo predictions are superimposed in dashed lines. Error bars for the experimental data are too small to be shown. In both cases, the Monte Carlo predicts a larger percent of the events upstream than indeed was found. This implies some problem with the modeling. The problem was that the incident K^o momentum sprectrum used for the Monte Carlo calculation had too large a contribution from large values. A low K^o momentum (P_K) associated event will have a larger $\pi^+\pi^-$ opening angle. Thus, in order to satisfy the aperature requirement of the A hodoscope, such an event must decay somewhat further downstream than the high P_K events. As a check on how sensitive the z spectrum was to the P_K spectrum, only the 2γ events for which $P_K < 2$ GeV/c were considered. The z distribution of these events is shown in Figure 26. The P_K cut drastically affects the z distribution by causing it to peak at the downstream end of the decay region. It is easy to see from these considerations that a slight variation of the P_K spectrum

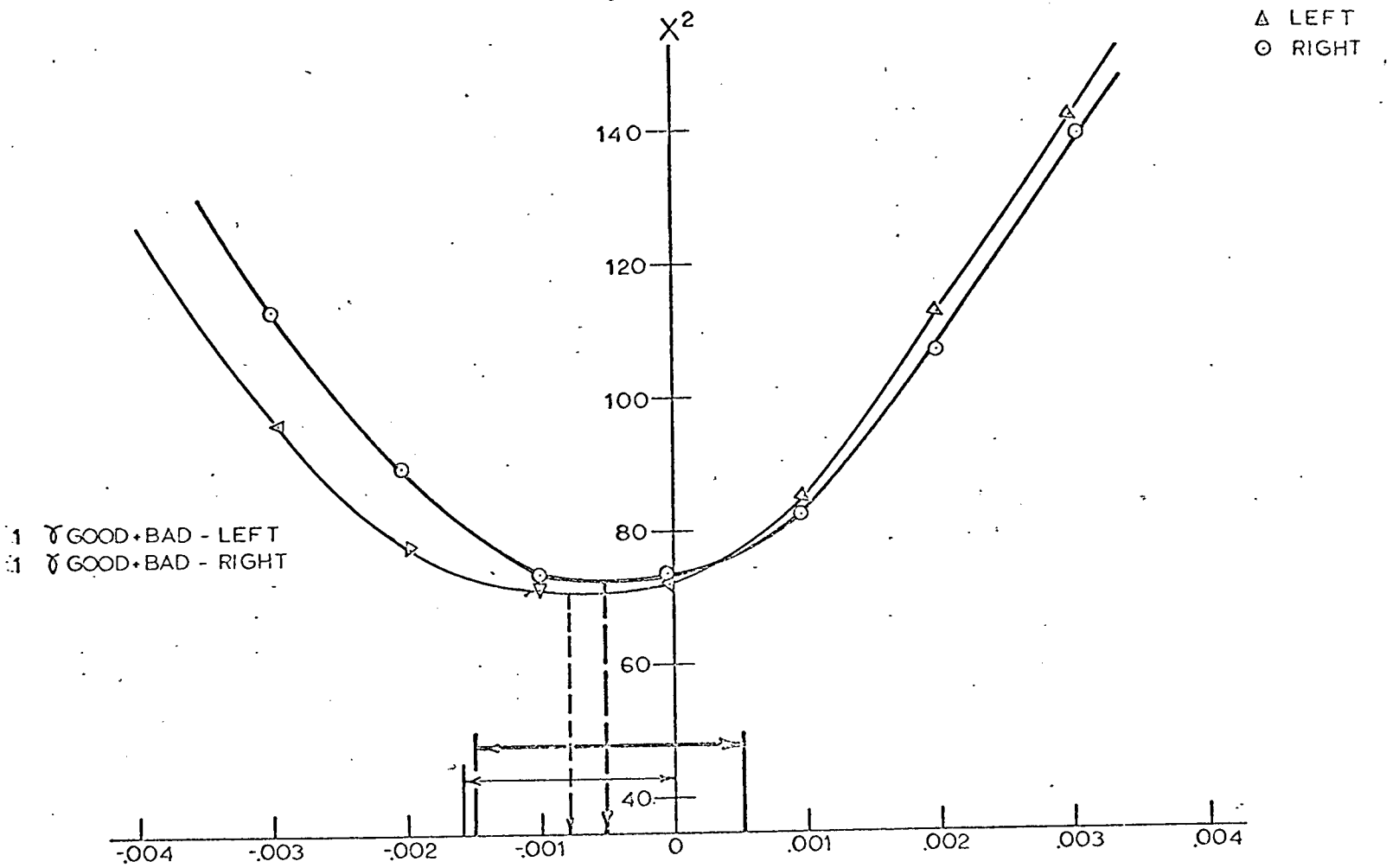

FIGURE 20
CHI SQUARED FIT TO THE ASYMMETRY FOR 1 γ (GOOD + BAD)

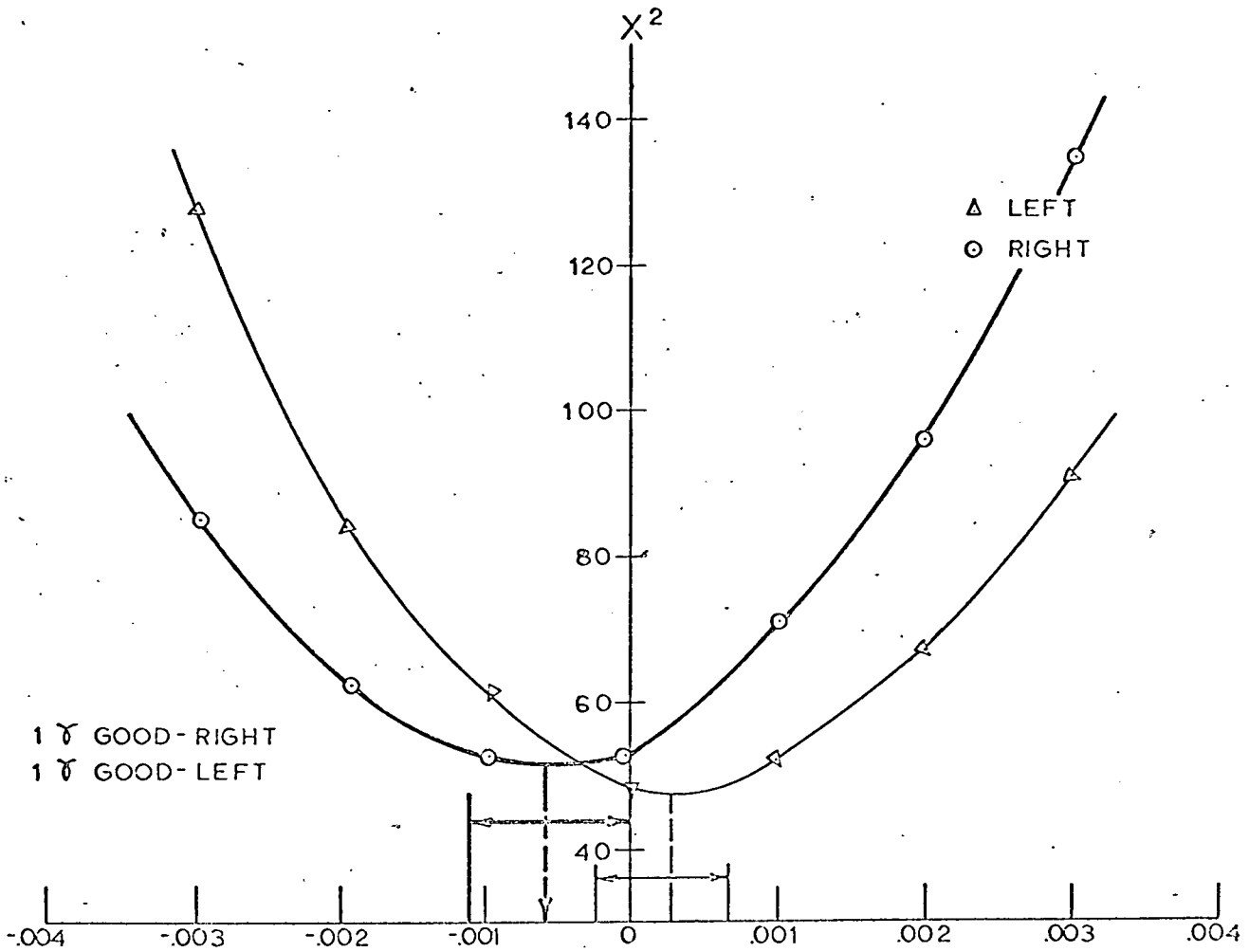

FIGURE 21
CHI SQUARED FIT TO THE ASYMMETRY FOR 1 γ (GOOD)

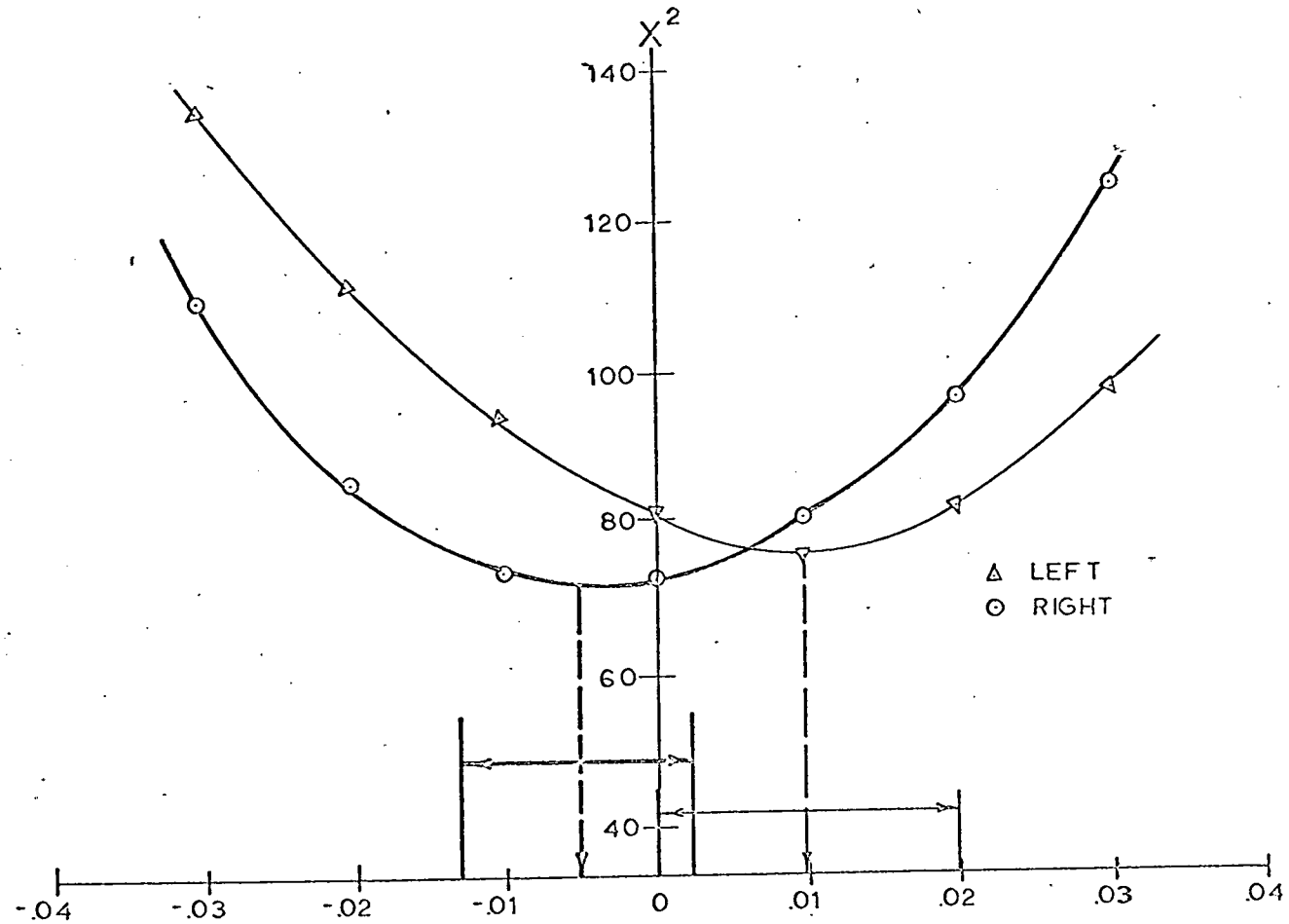

FIGURE 22
CHI SQUARED FIT TO THE ASYMMETRY 2 γ(GOOD + BAD)

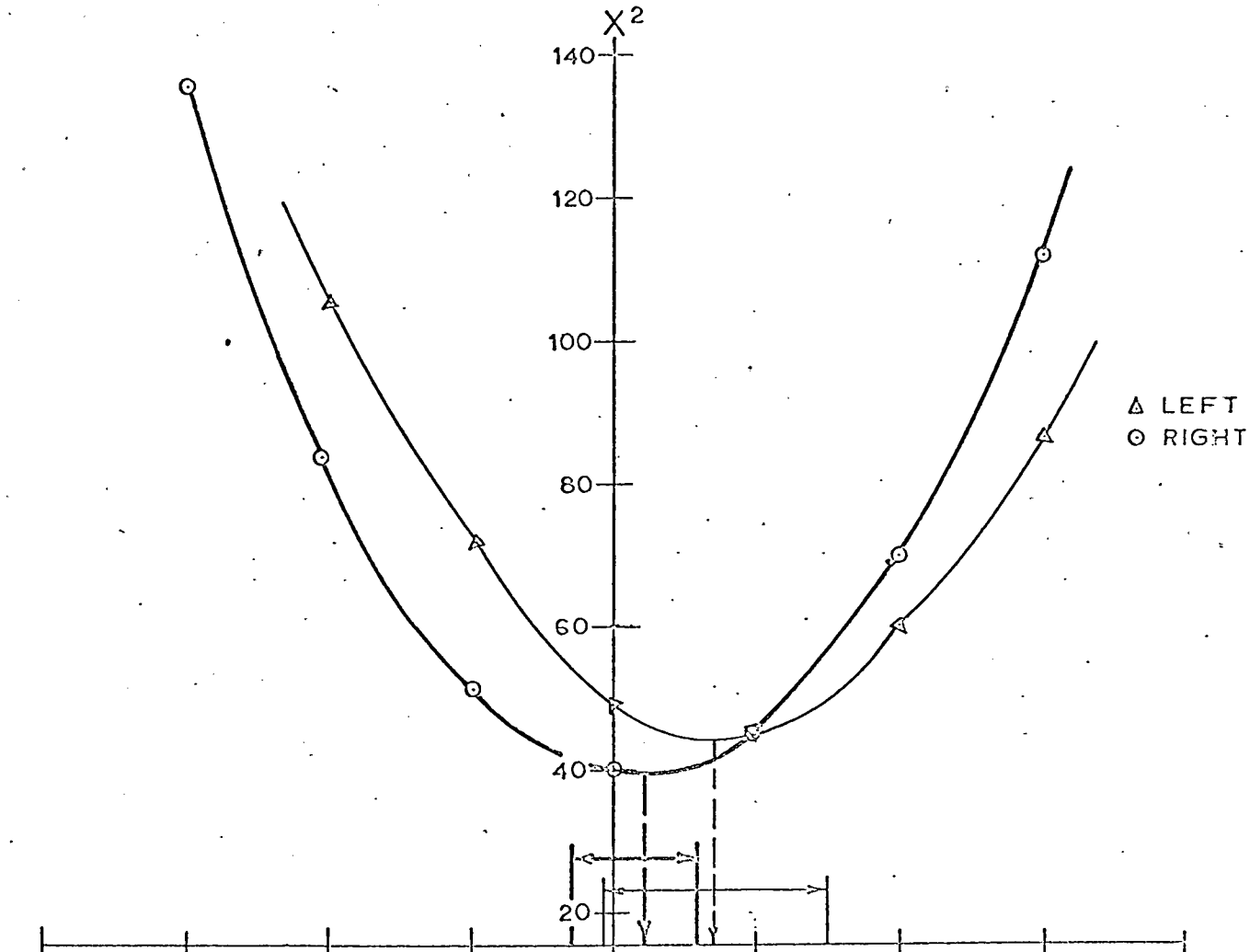

FIGURE 23

CHI SQUARED FIT TO THE ASYMMETRY FOR 2 γ (GOOD)

assumed would bring the Monte Carlo prediction into line with the experimental spectra. This variation in the Monte Carlo calculation does not affect the Monte Carlo prediction of the asymmetry spectra. As mentioned above, the asymmetry for $P_K < 2$ GeV/c were found to be the same as those for all Monte Carlo data.

I. Discussion of Systematic Biases

There are a number of sources of asymmetry that could reflect themselves in the data. Any such effects could cancel any true $\pi^+\pi^-$ asymmetry due to violations of CP symmetry. Such effects will be discussed in this section.

The effect of interactions of the beam with the apparatus itself was estimated by replacing the helium in the decay region with sulphur hexafluoride. This increased the amount of matter in the decay region (including the polyethylene bag) by a factor of 16. Since the count rate enhancement observed with the SF_6 was 30%, no more than 1.5% of the 1γ or 2γ events could be due to interaction processes. Since the asymmetry of the SF_6 (1γ) data was found to be no greater than 0.0015, the maximum possible contamination of the asymmetry due to interactions with the apparatus was 0.0006.

The profile of the incident neutral beam at the position of the apparatus together with the room background was experimentally determined in a previous experiment,[33] and implies that even if the background originating from interactions of beam particles with the

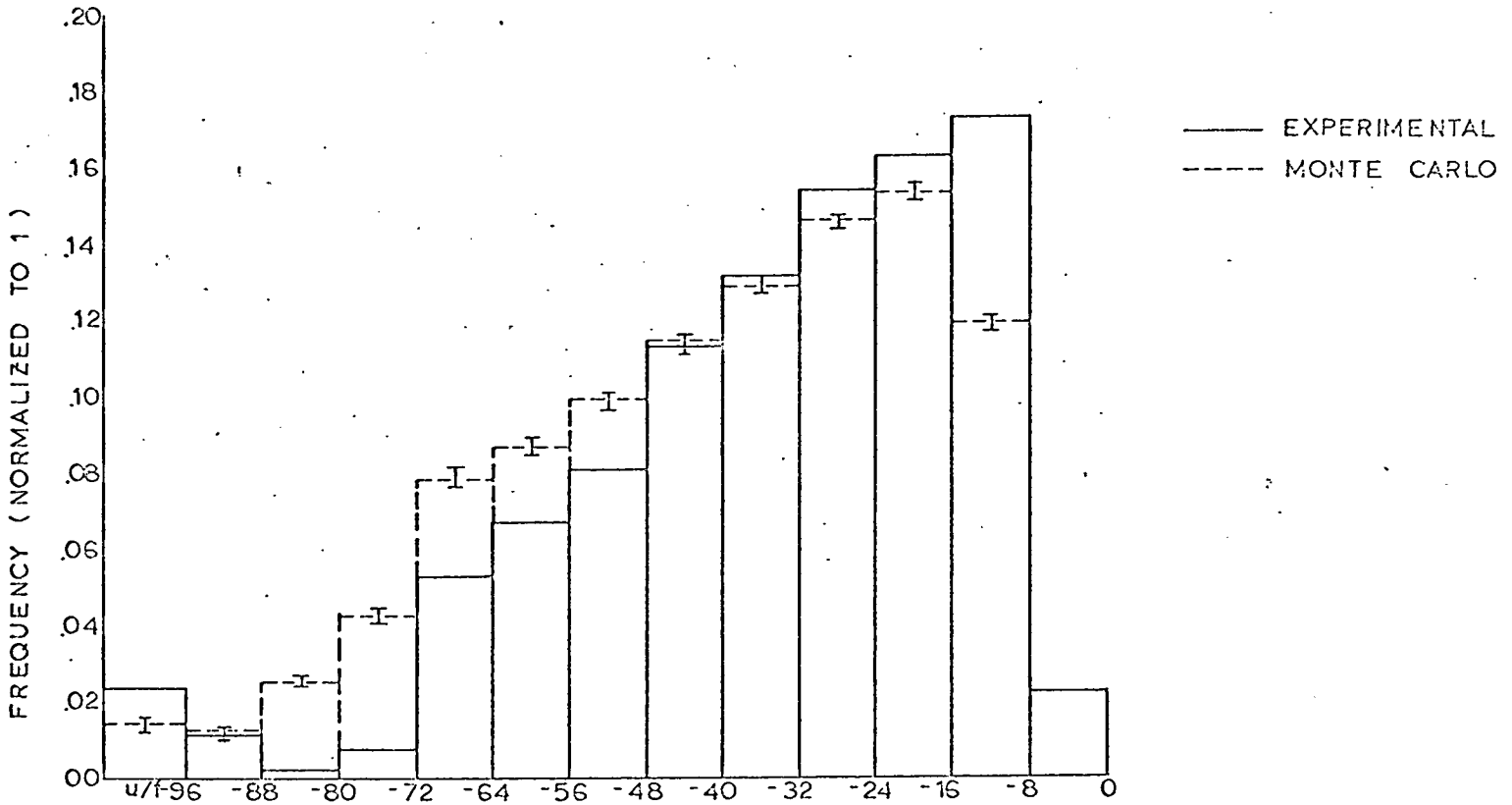

FIGURE 24
LONGITUDINAL DECAY POINT SPECTRUM 1 γ

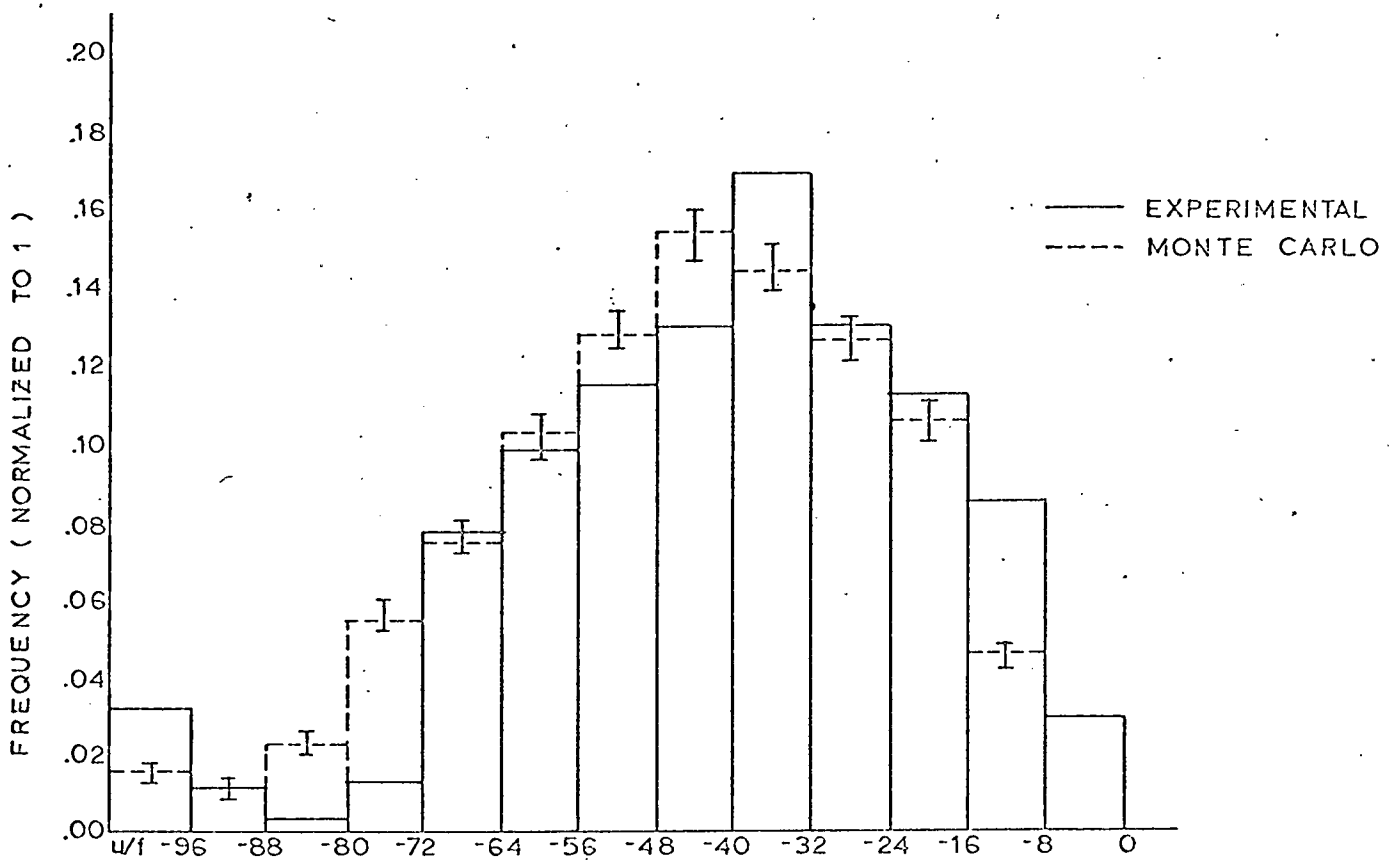

FIGURE 25
LONGITUDINAL DECAY POINT SPECTRUM 2γ

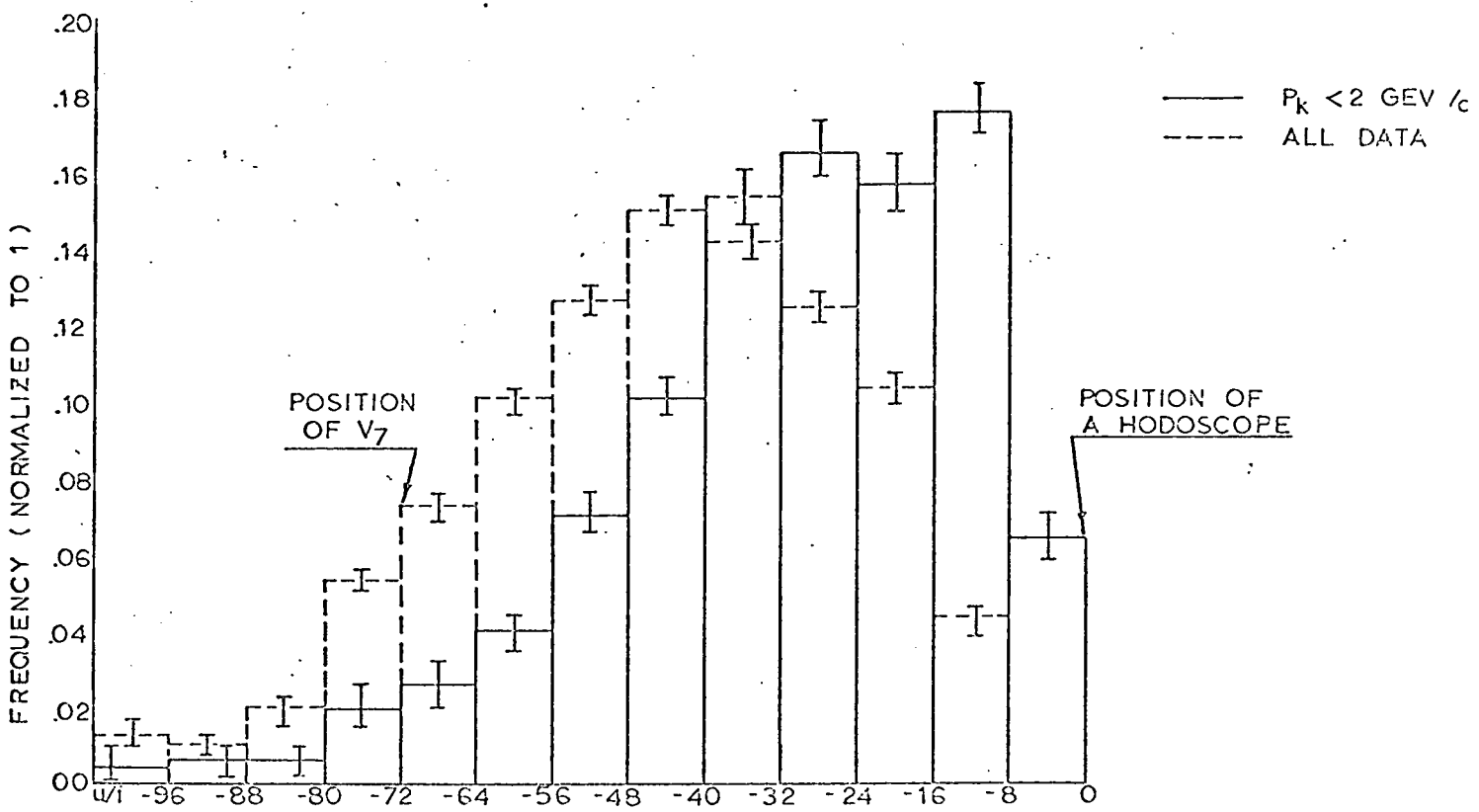

FIGURE 26
MONTE CARLO DECAY POINT SPECTRUM 2 δ

helium-bag walls and support structures were 100% charge asymmetric, their contributions to the measured $\sigma\pm$ would be smaller than 0.001.

Another possible source of masking asymmetry was due to the difference between the $\pi^+ - p$ and $\pi^- - p$ scattering cross sections. The average $\pi^+ - p$ scattering cross section is $\sim$ 100 mb. whereas for $\pi^- - p$ it is only $\sim$ 30 mb. for kinetic energies, T_π, of 0 to 400 MeV. For higher kinetic energies the cross sections are about the same. Thus, the events with a low T_{π^+} were scattered preferentially over those with a low T_{π^-}. To estimate the size of this effect, Monte Carlo data which assumed CP invariance was subjected to a kinetic energy cut. Using the standard Monte Carlo technique, events for which $T_{\pi^+} < 400$ MeV were "absorbed" with a probability of .3. A much higher absorption probability was used than the physical value of .003 in order to guarantee that the calculated stood out well above the counting statistics. Comparing the asymmetry generated by this technique with the Monte Carlo result for a true CP violation yields the limit $|\sigma\pm| \leq .0006$.

The analysis was performed separately for the data from the left side, and then the right. The results were then averaged. Since the asymmetry generated by magnet hysteresis was of opposite signs for the two data sets, the averaging cancelled the effect.

The systematic biases discussed above were included in the quoted uncertainty of $\sigma\pm$ by adding the contributions in quad-

rature with the uncertainty of the chi squared fit. The result of this operation is shown in Table 5. With the cut called "good", the results were .005 $\pm$ .006 for 2γ (good) events and .001 $\pm$ .0009 for 1γ (events).

J. Discussion of Results

The value obtained for σ_o was -0.2 $\pm$ 0.05. This agrees with values obtained by other experiments [34] and indicates that the chi squared and Monte Carlo analysis indeed is valid. It should be noted that the large uncertainty of this results is accounted for by the fact that the experiment was insensitive to the π^o energy.

The asymmetry parameter, $\sigma_{\pm}$, was found to be .0025 $\pm$ .008 for 2γ events, and -.0007 $\pm$ .0013 for 1γ events. The limit on $\sigma_{\pm}$ set by the 1γ (good) data is offered as the result of the experiment, because of its higher statistical precision.

The 1γ data were indeed due to $K_{3\pi}$, the decay of interest. Only decays of K_L^o could contribute significantly to the background. The decays with branching ratios large enough to be of concern are

$$K_L^o \rightarrow \pi^o\pi^o\pi^o \qquad (1)$$

$$K_L^o \rightarrow \beta^{\pm}\pi^{\mp}\nu \qquad (2)$$

$$K_L^o \rightarrow \mu^{\pm}\pi^{\mp}\nu \qquad (3)$$

Process 1 could contribute by the Dalitz decay of a π^o meson. These events would be effectively vetoed by the Cerenkov requirement. Processes 2 and 3 could contribute only by virtue of chance gamma coincidences. As discussed above, the chance gamma coincidence rate

was corrected for. Thus these processes did not represent significant contamination to either the 1γ or 2γ data.

The agreement of the Monte Carlo $1\gamma/2\gamma$ rate ratio of 11.2 with the observed ratio of 10.8 also suggests strongly the 1γ data indeed represent $K_L^o \to \pi^+\pi^-\pi^o$ decays. The shape of the 1γ momentum spectra agreed well with Monte Carlo 1γ spectra. These spectra are very sensitive to the decay kinematics, and, for example, are considerably different for 1γ events.

Thus, the 1γ data indeed represent the decay of interest and the data are sufficiently free of contamination that the 1γ result can be quoted. The best of the 1γ results is the 285,000 events that survived the cut "good", that is the 1γ (good). Thus,

$$\sigma\pm = .0001 \pm .0009$$

The results of this experiment are therefore consistent with CP invariance and the CP puzzle remains a mystery.

Case	Uncertainty
1γ (good+bad)	.0013
1γ (good)	.0009
2γ (good+bad)	.008
2γ (good)	.006

Table 5

Uncertainties of $\sigma\pm$ With Systematic Biases Included

REFERENCES

1. T.D. Lee and C.N. Yang, Phys. Rev. 106, 385 (1957).

2. C.S. Wu, E. Ambler, R.W. Haywood, D.D. Hopes, and R.P. Hudson, Phys. Rev. 105, 1413 (1956).

3. L.D. Landau, Nuclear Physics 3, 127 (1957).

4. T.D. Lee and C.N. Yang, Phys. Rev. 105, 167 (1957).

5. M. Gell-Mann and A. Pais, Phys. Rev. 97, 1387 (1955).

6. M. Bardon, K. Lande, L.M. Lederman, and W. Chinowsky, Am. Phys. 5, 156 (1958).

7. D. Neager, E.O. Okanov, N.L. Petrov, A.M. Rosanova, and V.H. Rusakoo, Phys. Rev. Letters 6, 552 (1961).

8. J.H. Christenson, J.W. Cronin, V.L. Fitch, and R. Turlay, Phys. Rev. Letters 13, 4, 138 (1964).

9. R.G. Sachs, Phys. Rev. Letters 13, 8, 286 (1964).

10. J.H. Christenson, J.W. Cronin, V.L. Fitch and R. Turlay, Phys. Rev. Letters, 13,4, 138 (1964).

11. G. Charpak and M. Gourdin, The $K^{o}\bar{K}^{o}$ System (CERN 67-18, 1967).

12. R.G. Sachs, Phys. Rev. Letters, 13, 8, 286 (1964).

13. Tran Truong, Phys. Rev. Letters, 13, 358 (1964).

14. T.D. Lee and L. Wolfenstein, Phys. Rev., 138, 6B, B1490.

15. J.H. Christenson, J.W. Cronin, V.L. Fitch, and R. Turlay, Phys. Rev. Letters 13, 138 (1964).

16. J.W. Cronin, P.F. Kuntz, W.S. Rish, and P.C. Wheeler, Phys. Rev. Letters 18, 25 (1967).

17. J. Prentki and M. Veltman, Phys. Rev. Letters 15, 88 (1965).

18. N. Cabbibo, Phys. Rev. Letters 14, 23 (1965).

19. P.K. Kabir, The C.P. Puzzle - Strange Decays of the Neutral Koan (Academic Press, Inc., London, England, 1968) p. 44.

20. T.D. Lee and C.S. Wu, Ann.Rev. Nucl. Sci. 16, 564 (1965).

21. Tran Truong, Phys. Rev. Letters 13, 11 (1964).

22. T.D. Lee and C.S. Wu, Ann.Rev. Nucl. Sci. 17, 153 (1966).

23. T.N. Truong, Phys. Rev. Letters 17, 153 (1966).

24. B.M.K. Nefkens, A. Abashian, R.J. Abrams, D.W. Carpenter, G.P. Fisher, and H. Smith, Phys. Rev. 157, 1233 (1967).

25. R.C. Smith, L. Wang, M.C. Whatley, G.T. Zorn, and J. Hornbostel, Bull, Am. Phys. Soc. 13, 586 (1968).

26. H.W.K. Hopkins, T.C. Bacon, and F.R. Eisler, Phys. Rev. Letters 19, 185 (1967).

27. B.M.K. Nefkins, A. Abashian, R.J. Abrams, D.W. Carpenter, G.P. Fisher, and J.H. Smith, Phys. Rev. 157, 1233 (1967).

28. S. Bennett, D. Nygren, H. Saal, J. Steinberger, and I. Sunderland, Phys. Rev. Letters 19, 7 993 (1967).

29. David M. Ritson, Techniques of High Energy Physics, Vol. V (Interscience Publishers, Inc., New York, (1961), p. 318.

30. S. Bennett, private communications.

31. R. Hagedorn, Relativistic Kinematics (W.A. Benjamin,Inc., New York, (1963), p. 112.

32. A.H. Rosenfeld et al UCRL 8030, Jan. 1968.

33. D. Nygren , private communication.

34. B.M.K. Nefkins, A. Abashian, R.J. Abrams, D.W. Carpenter, G.P. Fisher, and J.H. Smith, Phys. Rev. 157, 1233 (1967).

ACKNOWLEDGEMENTS

This experiment was a collaboration of high energy physics groups from McGill University, Harvard University, and Case Western Reserve University. All three universities helped to supply the manpower needed to set up and run the experiment. Discussions of the analysis procedure involved all three groups. The cooperation of the Physics Departments of Harvard University and McGill University is appreciated.

I would like to express my sincere thanks to my advisor, Professor William A. Blanpied, for his assistance and guidance through the initial stages of this research. I would also like to thank Professor Eugene Engels for advising me during analysis work at Harvard University.

I am obliged to Professor D. Keith Robinson for his aid in coordinating the writing of this thesis.

Thanks are due Doctors T. Kirk, M. Goitein, D. Stairs, and D. Ryan who helped during the execution of the experiment and contributed to the analysis of the data.

My gratitude is also due Professor J. Steinberger for making his apparatus available for this experiment, and to S. Bennett for his assistance with the PDP6 program.

R. Cool, J. Stanford, G. Tanguay and the staff of the Brookhaven Alternating Gradient Synchrotron are to be thanked for their fine cooperation.

I would like to thank Professor Thomas L. Jenkins for his advice and counselling over the past nine years.

I would like to express special thanks to Mrs. M. Young for her patience and labor in typing and coordinating this thesis.

Finally, I would like to thank my wife, Kathy, for her patience during my graduate career, and for her assistance in writing this paper.

This research was supported by the U. S. Atomic Energy Commission and the National Research Council of Canada.